INFORMATION TO USERS

This manuscript has been reproduced from the microfilm master. UMI films the text directly from the original or copy submitted. Thus, some thesis and dissertation copies are in typewriter face, while others may be from any type of computer printer.

The quality of this reproduction is dependent upon the quality of the copy submitted. Broken or indistinct print, colored or poor quality illustrations and photographs, print bleedthrough, substandard margins, and improper alignment can adversely affect reproduction.

In the unlikely event that the author did not send UMI a complete manuscript and there are missing pages, these will be noted. Also, if unauthorized copyright material had to be removed, a note will indicate the deletion.

Oversize materials (e.g., maps, drawings, charts) are reproduced by sectioning the original, beginning at the upper left-hand corner and continuing from left to right in equal sections with small overlaps.

ProQuest Information and Learning
300 North Zeeb Road, Ann Arbor, MI 48106-1346 USA
800-521-0600

HYDRODENITROGENATION OF PYRIDINE ON $NiO-WO_3-Al_2O_3$ CATALYST

by

Jamal Anabtawi

A Thesis submitted in partial fulfillment
of the requirements for the degree of

Master of Applied Science

to the

School of Graduate Studies
University of Ottawa
Ottawa, Ontario, Canada.

September 1977

ACKNOWLEDGEMENT

The author wishes to express his sincere appreciation and thanks to Dr. R.S. Mann for his guidance in carrying out this research work and his constructive suggestions in the preparation of this thesis; to Dr. J. Ruether for his help, to Dr. K.C. Khulbe and Mr. M. Dosi for their valuable discussions, to Mr. G. Gasperetti for his technical assistance and to Mrs. S. Roy for typing this thesis.

TABLE OF CONTENTS

LIST OF TABLES

LIST OF FIGURES

ABSTRACT

The kinetics of hydrodenitrogenation of pyridine over a catalyst containing 6% Ni and 19% W supported on alumina has been investigated in an integral fixed bed tubular reactor at 410 psig. The effect of various variables such as molar ratio, reaction temperature, initial partial pressure of reactants, and residence time on the conversion of pyridine have been studied. The reaction was carried out in a temperature range 120 - 380°C.

The reaction is believed to take place according to the following path:

pyridine $\xrightarrow[3H_2]{k_{ov}}$ piperidine $\xrightarrow[+H_2]{+pip}$ n-pentyl piperidine $\xrightarrow[+H_2]{-pip}$

pentane + ammonia

A rate equation for the first reaction namely, hydrogenation of pyridine has been suggested. Hydrogenation of pyridine to piperidine was found to be first order with respect to both pyridine and hydrogen. The apparent rate constant was found to be dependent on the initial partial pressure of pyridine.

The rate equation was formulated to be as follows:

$$-\frac{d}{dt}\left[P_{py}\right] = \left(k_i + k_s \bar{R} / \left[P_{H_2}^{\circ}\right]\right) \left[P_{py}\right] \left[P_{Hy}\right]$$

The activation energy of the reaction and the frequency factor were calculated to be 13.691 K cal /gm mole, and 5.987×10^{-2} $\frac{\text{gm-mole}}{\text{gm-cat-hr N/m}^2}$ respectively.

I. INTRODUCTION

The need for crude oil is increasing, while the resources are decreasing. For example, the United States has been conserving its crude by upgrading more of its distillate products at the expense of less valuable residiuum, but the yield of the residiuum cannot be reduced much more. Coal, shale oil, and tar sand will soon be used as raw material instead of crude oil, because they are more abundant (10). Hydrorefining and hydrocracking will be the essential steps in their upgrading to synthetic fuels.

The processing of these low grade raw materials poison the hydrocracking catalysts. While coal and shale oil contain nitrogen compounds Athabasca tar is very rich in sulfur compounds.

The function of a hydrocracking catalyst consists of hydrogenation, isomerization and cracking. By controlling and optimizing these functions, improvements in hydrocracking processes and their commercialization have been possible.

The principle role of a metal on a hydrocracking catalyst is to keep the acidic sites active throughout hydrogenation (21). They have profound effect on both the activity and selectivity.

The activity for hydrogenation is supplied by a metal deposited on a support, which is usually silica - Alumina. The principal role of the metal hydrogenation sites is to keep the acid sites clean and active by hydrogenating

the coke precursors, so that the area which is kept clean increases with the dispersion of metal on the acidic support (21).

Nitrogen as well as sulfur-containing compounds are known for their basic nature. Their presence in the feed stock could neutralize the acidic sites on the hydrocracking catalysts. However, with a high nitrogen feed stock the activity of the catalyst can be maintained by raising the temperature of the process.

Since, the activity is depressed by feeds that are high in nitrogen and sulfur, it is natural to consider hydrorefining of such feeds before hydrocracking. The difficulty of removing 'heteroatoms' increases in the order of oxygen, sulfur, and nitrogen.

Hydrodesulfurization and hydrodenitrogenation are the processes used to remove sulfur and nitrogen compounds from the feed. For example, the pyridines (and related quinolines) are hydrodenitrogenated to yield hydrocarbon and ammonia (17).

In Canada, the emphasis in the research program on "catalytic processing" at the Fuel research center, Department of Energy, Mines and Resources, is for the development of cheaper types of hydrosulfurization and hydrocracking catalysts for the upgrading of the heavy oils and tar.

Most of the studies of hydrodenitrogenation that are available in the literature refer to commercial catalysts.

The aim of these studies was to investigate the kinetics and find the optimum conditions of operation.

In this work, a kinetic study of pyridine hydrodenitrogenation over $NiO - WO_3 - Al_2O_3$ is reported and a possible reaction mechanism is postulated.

II. LITERATURE SURVEY

II-A Introduction

Nitrogen and sulfur compounds are universally present in fuels from shale oil, coal or lower grades of petroleum. The use of these sources soon will create a problem concerning the quality of the finished products. As mentioned before, nitrogen and sulfur compounds poison most of the modern catalysts used in refining and hydrocracking.

The majority of the work reported in the literature refer to the hydrogenolysis of thiophene and was undertaken to study the mechanism of desulfurization process. However, very little work has been published about the mechanism of hydrodenitrogenation process.

Hydrodenitrogenation was studied to understand the kinetics, the effect of the catalyst, and the optimum conditions for the reaction. In order to study hydrodenitrogenation, while some scientists used refinery stream such as: shale oil, heavy gas oil, tar etc. others used model compounds that are found in a refinery stream such as: indoles, quinoline, pyridine, pyroles, and amines.

Commercial catalysts were used to understand the way they function, and how to improve them. New catalysts were made to maximize the effect on the process of hydrodenitrogenation. The catalysts most frequently used are: $CoO - MoO_3 - Al_2O_3$, $NiO - MoO_3 - Al_2O_3$, $NiO - WO_3 - Al_2O_3$, and $NiO - WO_3 - SiO_2 - Al_2O_3$.

Most of the work done on hydrodenitrogenation was to understand the process as a whole for a definite set of conditions. For example, McIlvried (14) analyzed for the total nitrogen in the products. He assumed a scheme of reaction and derived a rate expression which could fit his experimental data.

Sonnemans et al. (15, 16, 17, 18) studied the hydrogenolysis of pyridine in detail. It was found that the reaction was not a simple one, but consisted of a complicated net work of reactions. Other effects, such as the rate of hydrogen circulation on the rate of hydrodenitrogenation, were studied (11). The interaction of hydrodesulfurization and hydrodenitrogenation has been also reported (12).

II-B Literature Survey

Cox (11) in a doctoral thesis studied the hydrodenitrogenation of pyridine and a number of pyridine derivatives. Toluene was used as a diluent in order to investigate nitrogen removal from a feed having 0.3% nitrogen by weight. The study was done at 700°F, 250 psig, with a space velocity of 0.5 to 20 ml/ml/hr. A previously hydrodesulfurized Peter Spence Cobalt - Molybdate catalyst was used. The catalyst (RD 3718), 1/8 inch by 1/8 inch had a composition: 2.5% Cobalt oxide and 14.% molybdenum oxide on alumina. Hydrogen flow rate was varied between 1000 scf/bbl and 7500 scf/bbl to ensure that the complete hydrogenation reaction was independent of hydrogen concentration.

With these two flow rates, two runs were made keeping all other variables fixed. No significant difference in nitrogen removal was observed.

Cox found a first order kinetics in pyridine to hold, and observed a decrease in the magnitude of the first order rate constant with increased concentration of nitrogen in the feed.

Flinn et al.(19) studied the hydrogenation of some pure nitrogen compounds such as amines, indoles, and quinoline over nickel - tungsten - alumina catalyst, and calculated the first rate constant for hydrodenitrogenation.

The kinetics of the hydrogenation of quinoline and some of its derivatives have been studied by Doelman et al. (20) using a Co - Mo - Al_2O_3 catalyst at a pressure of 80 atmospheres and a flow rate of 3000 normal liter/liter of feed and a space velocity of 1 liter solution/(liter of catalyst)/(hr.). The rate constants for the overall reaction were calculated.

The effect of cobalt to molybdenum ratios on desulfurization and denitrogenation has been studied by Williams et al.(3). An alumina supported cobalt molybdate catalyst containing 3% CoO and 13% MoO_3 was used. The effect of metal concentrations and atomic ratios on nitrogen and sulfur removal were also studied. The reaction was studied at a pressure of 2000 p.s.i., at temperatures ranging from 360 to 460°C, a liquid hourly - space velocity of 2.0, and a hydrogen flow rate of 5000 standard cubic feet per barrel.

It was found that higher the concentration of either of the component metals, higher was the amount of nitrogen removed. There was no optimum atomic ratio of cobalt to molybdenum.

Goudriaan et al. (4) studied the hydrodenitrogenation of pyridine over CoO-MoO-Al_2O_3 catalyst between 250 and 400°C at about 80 atm. pressure. It was reported that hydrodenitrogenation of pyridine was enhanced if the catalyst were presulfied rather than reduced. In the presence of hydrogen sulfide in molar excess over pyridine, the nitrogen removal was further increased. This was attributed to an enhancement in the hydrocracking activity of the catalyst by hydrogen sulfide.

Goudriaan (29), who investigated the hydrodenitrogenation of pyridine of NiO-WO_3-Al_2O_3 catalyst at 50 bar. pressure reported that while the hydrogenolysis of piperidine to consecutive products was the rate determining step below 350°C, at higher temperatures the hydrogenation of pyridine was the rate determining step.

Frost and Jensen (5) did hydrodenitrogenation tests on crude shale oil at 685, 740, 800°F at a pressure of 600, 1000, and 1400 psig., and a liquid space velocity of 0.1, 0.15, and 0.30 hr^{-1} in a flow reactor using a Co-Mo-Al_2O_3 catalyst.

Shale oil contains three major types of nitrogen compounds: quinolines, indoles and others. It was reported that the hydrogen partial pressure had a greater effect on

the denitrification rate constants of indole-type compounds than it did for either quinoline-type compounds or total nitrogen. At lower pressures and temperature relative denitrogenation constants were:

$$k_{de} \text{ total N} > k_{de} \text{ quinoline} > k_{de} \text{ indole}$$

while at higher pressures and temperature

$$k_{de} \text{ total N} = k_{de} \text{ quinoline} > k_{de} \text{ indole}$$

Agzamova et al (7) used a modified $Ni\text{-}Mo\text{-}Al_2O_3$ catalyst for the hydrodesulfurization and hydrodenitrogenation of gas oil and naphtha at 325°C, 40 bar. pressure, and a liquid space velocity of 1 hr^{-1}. The catalyst was modified with 1 wt % of unspecified metal. While sulfur and nitrogen removal was 36.89% and 18.0%, respectively for gas oil, it was 91% and 100% for naphtha.

The kinetics of the hydrodenitrogenation of pyridine in paraffin oil have been studied by Aboul-Gheit et al. (6) over $CoO\text{-}MoO\text{-}Al_2O_3$ catalyst at 350 - 400°C and an initial hydrogen pressure 25 - 100 atmospheres for 1 to 6 hrs. It was found that the reaction occurred in the following sequence: pyridine → piperidine → amylamine → pentane + ammonia. At lower temperatures alkyl-piperidines were formed in side reactions and their yield increased with the initial hydrogen pressure. Complete denitrogenation occurred only under the most severe set of reaction conditions.

Aboul-Gheit et al. (8) studied the hydrodenitrogenation of indole in paraffin oil over an alumina supported cobalt molybdate catalyst. The sequence of reaction was as follows:

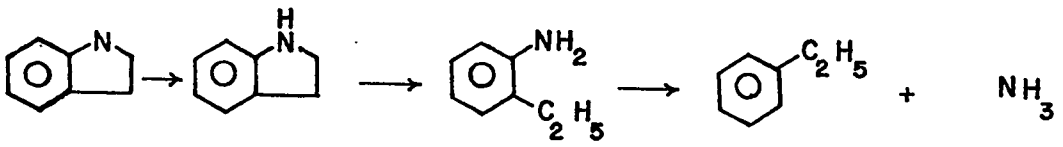

Indole indoline 0-Eth$C_6H_4NH_2$ Ethylbenzene ammonia

Best denitrogenation levels were accomplished at 400°C, 100 atmospheres initial hydrogen pressure, and a reaction time of 6 hrs.

The kinetics of the hydrodenitrogenation of quinoline in paraffin oil have been studied by Aboul-Gheit et al. (9) over a Co-Mo-Al_2O_3 catalyst at 350-400°C and an initial hydrogen pressure of 25-100 atmospheres for 1-6 hrs.

It was found that the reaction occurred in the following sequence:

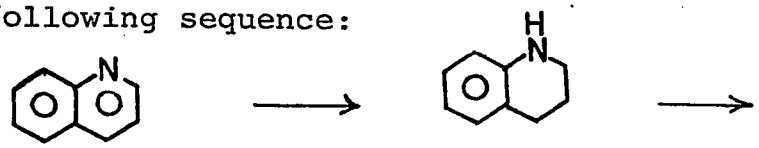

quinoline 1, 2, 3, 4 - tetranyaroquinoline

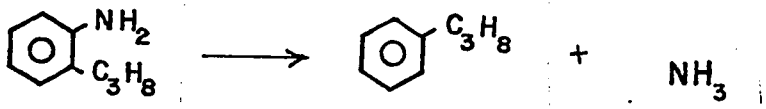

2 propylaniline propylbenzene ammonia

It was reported that denitrogenation was incomplete up to 400°C, an initial partial pressure of 100 atmospheres, and a reaction time of 6 hrs.

Satterfield et al (13) studied the effect of organosulfur compounds on the hydrodenitrogenation and the effect of organonitrogen compounds on the catalytic hydrodesulfurization. These two effects were investigated by using thiophene and pyridine as model compounds.

Studies were made in a continuous flow isothermal microreactor at temperatures 200 to 500°C and pressures of 4.4 and 11.2 bars over commercial $CoO-MoO-Al_2O_3$, $NiO-MoO-Al_2O_3$, $NiO-WO_3-Al_2O_3$ and $NiO-WO_3-SiO_2-Al_2O_3$ catalysts.

Satterfield suggested that pyridine hydrodenitrogenation took place according to the following scheme of reaction.

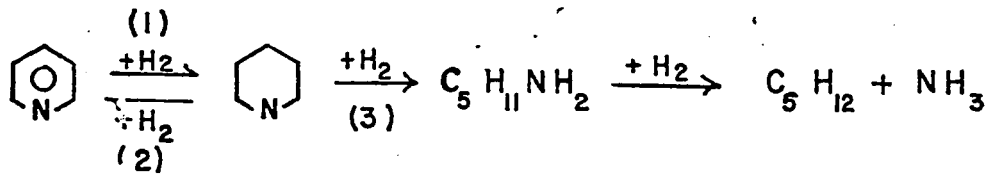

Sulfur compounds had a two fold effect on hydrodenitrogenation. At low temperatures, sulfur compounds competed with pyridine for hydrogenation sites on the catalyst, thereby inhibiting the reaction rate in step (1) in the pyridine decomposition mechanism. At high temperatures H_2S interacted with the catalyst to improve the hydrogenolysis activity, which increased the reaction rate for step (3) and resulted in an enhancement of hydrodenitrogenation reaction rate. Thus a maximum in the pyridine hydrodenitrogenation rate occurred at about 400°C and at 11 bars pressure over a commercial $NiO-MoO-Al_2O_3$ catalyst. This behavior was explained by considering the influence of the thermodynamic equilibria of steps (1) and (2) on the reaction. If step (1) was the rate determining step, piperidine formed would quickly react to products. However if steps (1) and (2) were fast relative to step (3) pyridine and piperidine could approach chemical equilibrium. Satterfield et al.(12) reported that an

equilibrium could be established between pyridine and piperidine at 430°C under the same conditions.

McIlvried (14) investigated the kinetics of hydrodenitrogenation of pyridine over a presulfided alumina supported catalyst containing 2.25% nickel, 1.25% cobalt, and 11% molybdenum. It was assumed that the reaction path occurred as follows:

pyridine → piperidine → n-pentylamine → pentane + ammonia

In order to understand the kinetics of the hydrodenitrogenation reaction, three sets of runs were made in a bench scale, fixed-bed, flow reactor, using solutions of n-hexylamine, piperidine, and pyridine in mixed xylenes. All runs were made at 600°F; pressure was varied from 750 to 1500 psig; nitrogen concentration in the feed ranged from 100 to 5115 p.p.m.; and space velocity ranged from 1 to 5.0 hr^{-1}.

It was reported that the path by which pyridine denitrogenation proceeded was through a rapid hydrogenation of pyridine to piperidine followed by slow-ring rupture to form n-pentylamine and a rapid denitrogenation of n-pentylamine to ammonia and pentane.

It was assumed that all nitrogen compounds involved were equally strongly adsorbed on denitrogenation sites or else their concentrations were too small to have a significant effect on the kinetics of reaction. Denitrogenation data obtained with piperidine was found to fit a Langmuir-Hinshelwood-type kinetic model. This rate expression was then used to develop an equation which fitted the data for pyridine

denitrogenation.

The hydrodenitrogenation of pyridine followed a first order kinetics in pyridine and a first order in hydrogen as shown by the rate equation:

$$-\frac{d}{dt}\left[P_{py}\right] = \frac{455\,\pi\,\left[P_{H_2}\right]\left[P_{py}\right]}{(1-\bar{R})(1-10.5)\left[P_{Am}\right]} \times 10^{-4}$$

The mechanism of the hydrogenolysis of pyridine has been investigated by Sonnemans et al. (15) over a presulfided alumina - supported $CoO-MoO_3$ catalyst by measuring the kinetics at low and high hydrogen pressures. Conversions of pyridine, piperidine and n-pentylamine were studied as a function of reaction time, partial pressures of the reactants, temperature and catalyst type. From the results obtained a reaction scheme was derived in which three types of reactions were observed: hydrogenation, cracking and disproportionation. Hydrogenation and disproportionation reactions appeared to have higher reaction rates than cracking reactions.

To understand the function of cobalt, molybdenum and alumina oxide towards the different types of reactions (hydrogenation, cracking, disproportionation) the rates of conversion of pyridine, piperidine and n-pentylamine were determined on various catalysts. Molybdenumoxide was the active component for the different types of reactions. The alumina surface apparently did not contribute to the activity.

Sonnemans et al. (16) studied the mechanism of pyridine hydrogenation on a $MoO-Al_2O_3$ and $CoO-MoO-Al_2O_3$ catalyst at high hydrogen pressures. The reaction order in pyridine was determined by changing the residence time and the initial partial pressure of pyridine. Hydrogenation of pyridine was found to follow a first order in pyridine. However, the first order rate constant appeared to be inversely proportional to the initial partial pressure of pyridine.

The following reaction scheme was assumed to occur with the purpose of determining the order of reaction with respect to hydrogen

$$3H_2 + \text{pyridine} \underset{k_{-1}}{\overset{k_1}{\rightleftharpoons}} \text{piperidine} \overset{k_c}{\rightarrow} C$$

The rate determining step of these two reactions determined the order in hydrogen.

The kinetic rate equation of hydrogenation of pyridine was derived.

$$-\frac{d\left[P_{py}\right]}{dt} = k_{ov}\left[P_{py}\right]\left[P_{H_2}\right]^m$$

where m = 1 at 250°C

m = 1.5 at > 300°C

The adsorption behavior of nitrogen bases and hydrogen on alumina and molybdenum - containing catalysts was investigated by the gas chromatographic methods. The adsorption of the nitrogen bases appeared to be very strong on both catalysts, and varied in the order piperidine >

pyridine > ammonia.

Hydrogen also showed strong adsorption. Hydrogen and nitrogen bases appeared to adsorb on different sites.

The kinetics of the conversion of piperidine has been investigated by Sonnemans et al. (17) on $CoO-MoO_3-Al_2O_3$ catalysts at a hydrogen pressure of 60 atmospheres. Piperidine conversion was studied as a function of temperature, initial piperidine partial pressure, reaction time and initial hydrogen pressure. It was reported that n-pentylpiperidine was a major intermediate in the conversion of piperidine to ammonia and pentane. n-Pentylpiperidine was formed by alkyl transfer from n-pentylamine to piperidine. Several compounds were analyzed in the product stream such as: dipentylamine, pentene and decane. A reaction scheme was postulated as follows:

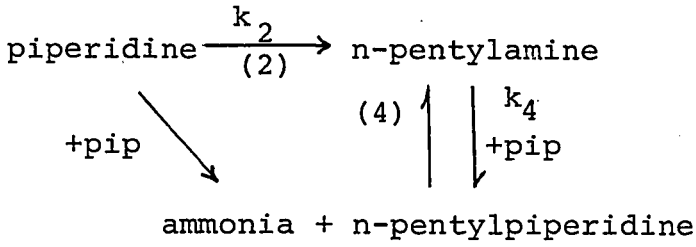

The conversion of piperidine to ammonia and pentylamine was described by two steps: a slow reaction (2) followed by a fast reaction (4). Hence, at hydrogen pressure of 60 atmospheres and conversion below 50%, piperidine was selectively converted to ammonia and n-pentylpiperidine. This reaction was a two steps process, ring opening to n-pentylamine followed by fast alkyl transfer from n-pentylamine to piperidine. The rate equation for hydrocracking

was derived:

$$r = k_h \left(\left[P_{pip}\right] / \left[P^{\circ}_{pip}\right] \right) \left[P_{H_2}\right]$$

At conversions higher than 50%, the rate of formation of pentane and ammonia was influenced by the rate of hydrocracking steps, and also by the equilibrium constants of the alkyl transfer equilibria. The rate equation for the alkyl transfer reaction was given by

$$r = k_a \left(\left[P_{pip}\right] \left[P_{mpa}\right] / \left[P^{\circ}_{pip}\right] \right)^2 \left[P^{\circ}_{H_2}\right]$$

Sonnemans et al (18) studied the conversion of pentylamine over a MoO $-Al_2O_3$ catalyst between 250 and 350°C, at various hydrogen pressures. The reaction observed were cracking to pentene and ammonia, hydrocracking to pentane and ammonia, dehydrogenation to pentanimine and butylcarbonitrile, and disproportionation to ammonia and dipentylamine.

The equilibrium between pentylamine, dipentylamine and ammonia appeared to be established under most experimental conditions. A first order dehydrogenation of n-pentylamine to butylcarbonitrile was observed at hydrogen pressures of 1 atm. and less. The selectivity of the pentylamine conversion in this compound increased at increasing temperatures. The disproportionation reaction was found to follow a zero order in hydrogen and a -1 order in the initial n-pentylamine pressure.

Both cracking and hydrocracking took place mainly above 300°C. While hydrocracking appeared to be 0.5 order in hydrogen, cracking was zero order in hydrogen. The order

in n-pentylamine was zero order for both cracking and hydrocracking.

II-C Objectives of this work

A systematic study was undertaken on the hydrodenitrogenation of pyridine over $NiO-WO_3$ on Al_2O_3 catalyst with the purpose of:

1. Understanding the hydrodenitrogenation of pyridine on $NiO-WO_3-Al_2O_3$ catalyst as an example of hydrodenitrogenation process.
2. Studying the reaction scheme of hydrogenolysis. The products formed from pyridine at high hydrogen pressure were determined as a function of temperature while keeping the reaction time constant.
3. Investigating the effect of the process variables such as reactant ratio, space velocity and temperature on conversion and product distribution at moderate higher pressures of hydrogen over $NiO-WO_3-Al_2O_3$ catalyst.
4. Developing a suitable rate expression and of postulating a reaction mechanism which might represent the experimental data.
5. Calculating a rate constant for the hydrogenation of pyridine, activation energy and Arrhenius constant.

III. EXPERIMENTAL

Schematic Diagram of Experimental Apparatus

Symbol	Item
H_2	Hydrogen supply
He	Carrier gas
PR	Pressure regulator
DM	Drier and Molecular sieve
PG	Pressure gage
R	Reactor in fluidized sand bed
TC	Thermocouple
FF	Fluid bed furnace
VP	Valves to reduce pressure to one atmosphere
GSV	Gas sampling valve
CT	Cold trap
RC	Reference column
S.C	Sample Column
G.C	Gomac Cell
RE	Recorder
WT	Wet test meter
F	Vessel with liquid feed
P	Pump
RO	Rotameter
C	Condenser

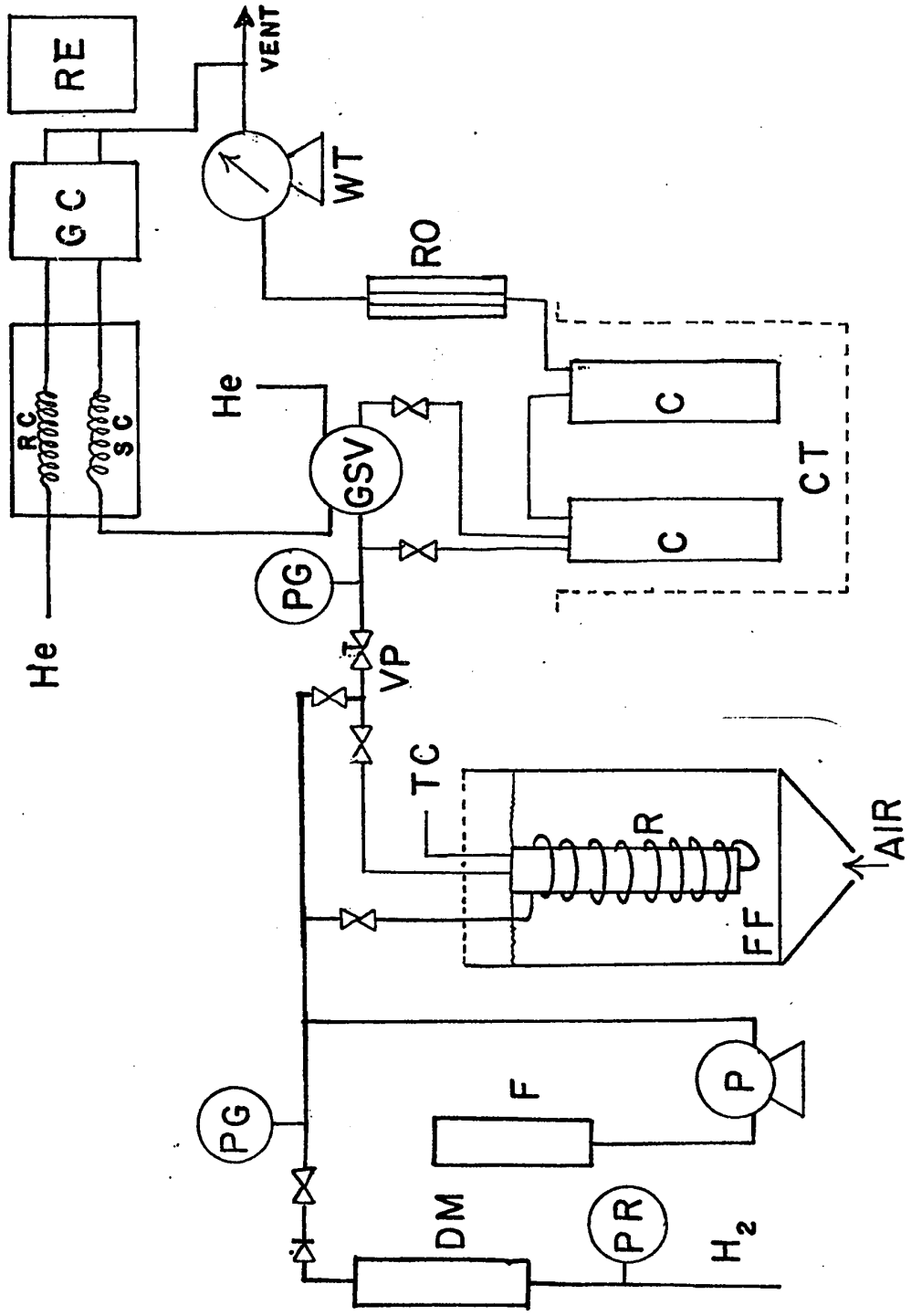

Fig. 1 Shematic diagram of experimental apparatus

III-A Description of Apparatus

The hydrodenitrogenation of pyridine was carried out in a fixed-bed, bench scale, flow system. The high pressure apparatus was designed to operate at a controlled temperature and pressure. A schematic diagram of the apparatus is shown in Figure (1).

The apparatus may be divided into three sections: (i) Feed of reactants, (ii) Reactor assembly, and (iii) Product analysis unit.

(i) Feed section:

This section consisted of four gas streams and a pyridine feed system. Two gas streams supplied helium as a carrier gas to the reference and sample columns. Helium was obtained from a high pressure cylinder through a two stage pressure regulator, a drying tube packed with drierite (Fisher Cat. No. C-140) and then through flowmeter (tube and float series 601, Matheson Co.). The gas lines used for helium were ¼" O.D. Copper tubing. The third stream, which carried air to the sand bed, was ¼" O.D. copper tubing. The fourth stream carried hydrogen from a high pressure cylinder through a pressure regulator (Model - 2 catalogue no. CGA-2, Matheson Co.). Traces of moisture, and other impurities from hydrogen were removed by passing it through a stainless steel tube packed with drierite and molecular sieve. The gas lines for hydrogen

were made of ¼" O.D. stainless steel tubings. A unidirectional valve Nupro check valve (cat. no. SS-2C-10, supplied by Ottawa Valve & Fitting Ltd., Ottawa) was used to control the direction of hydrogen flow. 2 ft. before mixing with pyridine, the hydrogen line was heated by wrapping around it a ½" wide heating tape (supplied by Fisher Cat. no. 11-463-40A).

The pyridine feed system consisted of a mini pump (Model 396-31, Milton Roy Industries, Peterborough, Ont.). The flow rate of pyridine could be varied by adjusting the percentage stroke. Pyridine was carried to the reactor by a 1/8" O.D. stainless steel tubing. Pyridine was vaporized and maintained as such by heating the tube externally by a heating tape. The heating tape was used to cover all tubing until the cold trap to avoid condensation of the liquid products. Asbestos wrap cloth tape (supplied by Fisher catalogue no. 1-473 A) was used to prevent heat loss from the system.

(ii) Reactor Assembly:

The reactant stream was connected to a two ways valve, while one branch led to the reactor through a preheater the other by passed the reactor and preheater. The preheater was made of 6 feet long 1/8" O.D. 316 stainless steel tubing which was wound around the reactor. The preheated reactants

entered from the bottom of the reactor. The reactor was 8" x ½"O.D. 316 stainless steel tube. A porous stainless steel plate (supplied by Pall Trinity Micro Corp., Cortland, New York) was fixed at the bottom of the reactor tube. The grade D plate had a mean pore size of 65 microns, a normal thickness of 1/16 inch and produced a pressure drop of approximately 0.1 psig per 180 cfm / sq. ft. of hydrogen. An autoclave reducer was welded below the porous plate and connected to the feed line from the preheater.

The top of the reactor was connected to swagelok "T" connection (SS-400-3) through a ½" to ¼" reducer union. Through the upper opening an iron constantan thermocouple was inserted. The lower end of the thermocouple tube was kept just above the porous plate in contact with the catalyst bed. The thermocouple was connected to a millivolts polentiometer (supplied by Jones G. Biddle Co., Plymouth Meeting, PA.) for measuring the temperature during the reaction. The thermocouple was supplied by Thermoelectric Canada Ltd., Brampton, Ontario). A second iron constantan thermocouple was inserted in the fluidized sand bed. The temperature of the reactor was controlled by a Honeywell pyr-o-vane temperature controller. It was used with tranducers such that the output signal from the second thermocouple was

measured by the controller which activated the relay to maintain the temperature constant at the set point. The controller when coupled with an energy regulator (Fisher catalogue no. 9-521-130) could maintain the reactor temperature to $\pm$ 2°C.

The reactor and the preheater of reactants were kept immersed in a constant temperature fluidized bed furnace. The container for the fluidized bed was made from a 6 inch O.D. steel cylinder. A porous stainless steel plate (Pall Trinity Micro Corp., Cartland, New York) was inserted at the bottom and further welded to a reducing cone with ½" pipe. Clean sand 40-60 mesh size was used as the heating medium of the fluidized bed, and was placed in the container on top of the porous plate. The reactor was held upright in the center of the bed. Sufficient flow of air was passed to keep the sand fluidized and to obtain a uniform temperature around the reactor.

For heating the reactor, two layers of ceram-A-flex beaded heating wire (Chemical Rubber Co., Cleveland, Ohio) were wrapped around the steel cylinder. A paste of asbestos powder mixed with water was applied to the wires for insulation and to fix the wires in position. The asbestos was left to dry slowly to prevent cracking. The inner heating wire was connected to the temperature controller. The

external heating wire was connected to a 10 ampere power-stat (Fisher catalogue no. 9-521-130) and was adjusted to a sufficient power to maintain the reactor temperature slightly below the required temperature set on the temperature controller. This reduced the heating load in the controller circuit (inner heating wire) and more precise control of the reaction temperature was made possible. The reactor and fluidized bed were placed in an outer steel cylinder 12 inches in diameter, placed on a piece of asbestos plate, in the centre of which a hole was provided for air line to fluidize the bed. The annular space between the steel cylinder and the bed was packed with wet asbestos powder.

(iii) Product Analysis Unit:

This section of the apparatus consisted of a liquid trap, two condensers, gas sampling valve, rotameter, wet test meter, gas chromatographic equipment for the product analysis, and a recorder. The products from the reactor pass through a high temperature gas sampling valve (cat. no. V-8-Ht, Chromatographic Specialties Ltd., Brockville, Ont.) which was kept at 140°C by a heating tape controlled by an adjustable energy regulator (Fisher cat. no. 9-521-130). The gas sampling valve had 8-ports. The carrier gas continuously passed through the first loop (1 ml)

while the product stream passed through the other loop (1-ml). When the sampling valve was turned on, the flow of the product stream and the carrier gas were switched. A certain volume of product stream was flushed by helium to the sample column for analysis. The pressure on the sample loop was kept constant at each injection to be sure that a constant volume was injected each time. This was done by adjusting the flow before and after the gas sampling valve. The product stream after leaving the gas sampling valve entered into two liquid traps which were cooled in an ice bath. The heavier reaction products such as piperidine and n-pentyl piperidine and unreacted pyridine were condensed. Hydrogen and other gaseous products passed through a rotameter with (tube and float series 601, Matheson Co.) before going to the vent. The product stream passed through a precision wet-test meter (supplied by Precision Scientific Co., Chicago, U.S.A.) where the flow rate was measured.

A Gow Mac W-2X hot wire, 333 mount, made of rhenium-tungsten, in a temperature regulated four element macrocell (Model TR-III AWX) was used to analyze the products separated by the column. The temperature was constantly maintained at 170°C. The detector temperature was controlled by a Fenwal Thermo switch with an adjustable range from ambient

to 205°C. Two cartridge heaters were connected in series with a thermoswitch and the temperature of the unit could be varied by turning on adjustable screw at the bottom of the case, one revolution clockwise for every 32°C rise in temperature and vise-versa.

Direct current for the detector was supplied by a Gow Mac Model 405-C : 1 Solid State DC power supply with an input power of 115 volts A.C. at 60 cycle per second and output power from 0 to 40 volts A.C. The regulated output ranged from 0 to 500 ma. with a four steps voltage control starting at 6-10 volts.

The output signal in millivolts from the detector was transferred to a chart recorder (Texas Instrument Inc., Texas model Serva/ritter II).

III-B Calibration of Equipment

Flow rates of gas stream were measured by calibrated rotameters. The volumetric flow rates were checked by the wet test gas meter supplied by Precision Scientific Co. A correction for the temperature difference of the gas stream from the room temperature was necessary.

Calibration of the pump was done by connecting a two-ml graudated pipet to the pump. For each pump setting in percentage stroke, a corresponding rate in volume of pyridine per unit time was measured. A calibration curve is given in figure (3).

For the calibration of the gas chromatograph, pure compounds that are expected to form as well as pyridine are

analyzed in the vapor phase. The order of elution was recorded. Synthetic mixtures of these compounds were made. The chromatograms of these mixtures were taken. The area under the peak of each component was calculated. A calibration curve indicating the number of moles of component against the area under the peak was prepared.

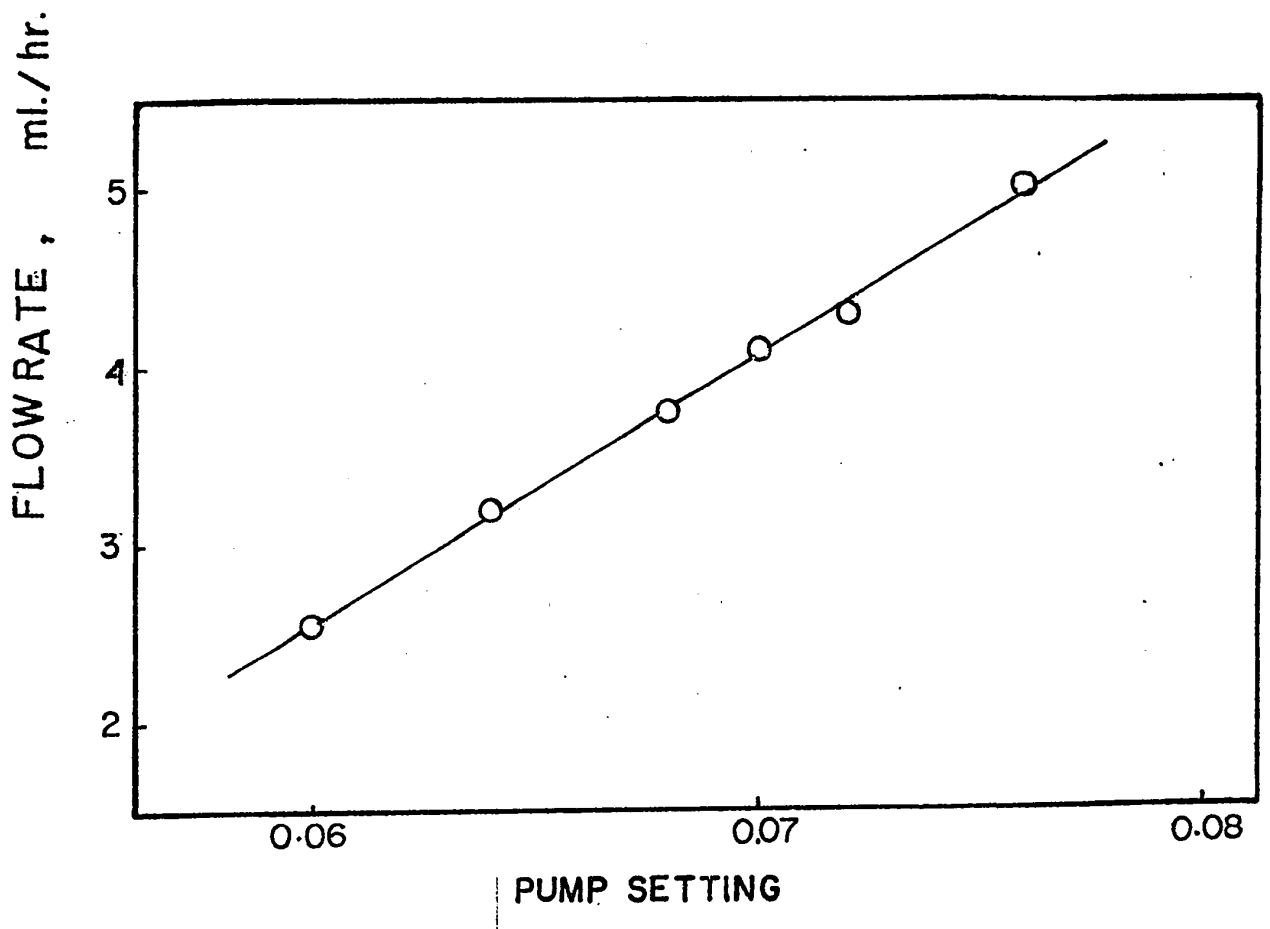

Fig. 3 Calibration of the pump

III-C Analysis Procedure

A thermal conductivity detector was used in the analysis of the various components of the reaction product. A column packed with 10% (w/w) carbowax 1000 coated on a solid support was used to separate the products. Chromosorb W/AW 60-80 mesh, coated with 10% NaOH (w/w) with the aid of NaOH solution was used as the solid support (22). Two columns each five meters long were used in parallel to give a stable base line in the recorder. Temperature programming was necessary. The column temperature was raised to 40°C at which ammonia and pentane were separated within 3 minutes. The temperature then was raised to 120°C at a rate of 20°C/ minute. The flow rate of the carrier gas was 80 ml / minute.

III-D Experimental Procedure

Start Up and Operation

The following are the steps that were necessary in the start up and operation of the equipment.

(i) The catalyst was weighed and placed in the reactor.

(ii) The reactor was reassembled and checked for any leaks while outside the fluidized bed.

(iii) If there was no leak in the reactor, the apparatus was checked for any leaks by applying a pressure of 600 psig and left for 3 hours after closing the inlet and the outlet valves. If there was a pressure drop, the apparatus was checked for pressure drop in each section. The leaking section was checked with soap solution.

(iv) Temperature was set at 450°C, the furnace was switched on and hydrogen flow was adjusted. The system was then left for 48 hrs to activate the catalyst.

(v) Temperature was set at the required temperature and then left for 12 hours so that the temperature stabilized.

(vi) Helium flow was checked, the detector and recorder were switched on.

(vii) Hydrogen flow rate was adjusted and left for one hour at the adjusted flow rate.

(viii) The pump was set at a given flow rate and switched on.

(ix) Ice was placed in the ice bath.

(x) Three samples were injected after 2 hours from starting the pump. The injections were repeated until consistency of the peak heights was obtained.

(xi) The first run carried over a fresh catalyst was repeated two weeks later to check for the activity of the catalyst. The catalyst was changed every three weeks or so.

III-E Reactants and Chemicals

The catalyst used was supplied by the Department of Energy, Mines and Resources. It was Ni-4303 made by Harsaw Chemical Co.. Although the catalyst was supplied as 1/8" extradate it was crashed and screened to provide 20-40 mesh granules.

Hydrogen and helium were supplied by Oxygen of Ottawa Ltd., Ottawa. Pyridine and other chemicals used for calibration were supplied by Fisher. These chemicals were used without any further purification.

The chemicals used in the preparation of Gas Chromatographic Columns, chromosorb W/AW 60-80 mesh and carbowax 1000 cat. (no. SPA46) were supplied by Chromatographic Specialties Ltd., Brockville, Ontario.

IV. RESULTS

The experimental data was obtained by means of an isothermal fixed bed reactor operated at a pressure of 2.928 x 10^6 N/m^2. A period of 2 hours was considered enough to reach steady state. A further confirmation was obtained from the product analysis.

The effect of various variables, namely, molar ratio of hydrogen to pyridine ($\bar{R}$), reaction temperature (T), and the ratio of the catalyst weight in gms to the total feed in moles/hr (W/F), on the conversion of pyridine (X) have been studied.

The conversion (X) was defined as the ratio of moles of pyridine reacted per hour to the moles of pyridine fed per hour into the reactor.

The reaction scheme for the hydrogenolysis of pyridine was achieved by studying the effect of temperature on conversion and product distribution in the range of 120 - 380°C. The reaction time (W/F) and the molar ratio ($\bar{R}$) were kept constant. The amount of products formed were expressed as (moles product)/(moles of pyridine in the feed). The effect of temperature was repeated for three different mole ratios ($\bar{R}$), keeping the reaction time constant. Tables 1-4 show experimental data of (moles prod.)/(moles of pyridine in the feed), at W/F = 3.6 gm-cat-hr/gm-mole, in the range of 120 - 380°C at mole ratios $\bar{R}$ = 29, 40, 60 and 80.

Figures 5-8 show the effect of temperature on the product distribution with $\overline{R}$ as a parameter. It can be seen that piperidine was the only product at low temperatures. As the temperature increased an intermediate product (n-pentyl piperidine) was formed. N-pentyl piperidine decomposed into pentane and ammonia. At smaller mole ratios other products such as: pentene, n-pentylamine, dipentylamine and decane were formed, but in small quantities. The set of curves shifted to the left as the mole ratio of hydrogen/pyridine increased.

The effect of mole ratio on the conversion, with temperature as a parameter, was investigated for pyridine and the products. At a certain temperature conversions were obtained for various mole ratios. Conversion of pyridine was defined as ratio of moles of pyridine reacted per hour to the moles of pyridine fed per hour into the reactor. For the products, the rate of formation was defined as moles of product formed per hour to the moles of pyridine fed per hour into the reactor. The calculated data for the effect of mole ratios on the conversion at various temperatures is given in Tables 5-9. The conversion (X) against mole ratio $\overline{R}$ (Figures 9-13) plots show that conversion (X) varies linearly with mole ratio ($\overline{R}$).

The effect of various W/F ratios on the conversion of pyridine was investigated in the range of W/F = 2.09 to 9.45 gm-cat-hr/gm-mole and at temperatures 145, 195, 245 and 280°C for hydrogen/pyridine mole ratios of 40, 50, 60 and 90.

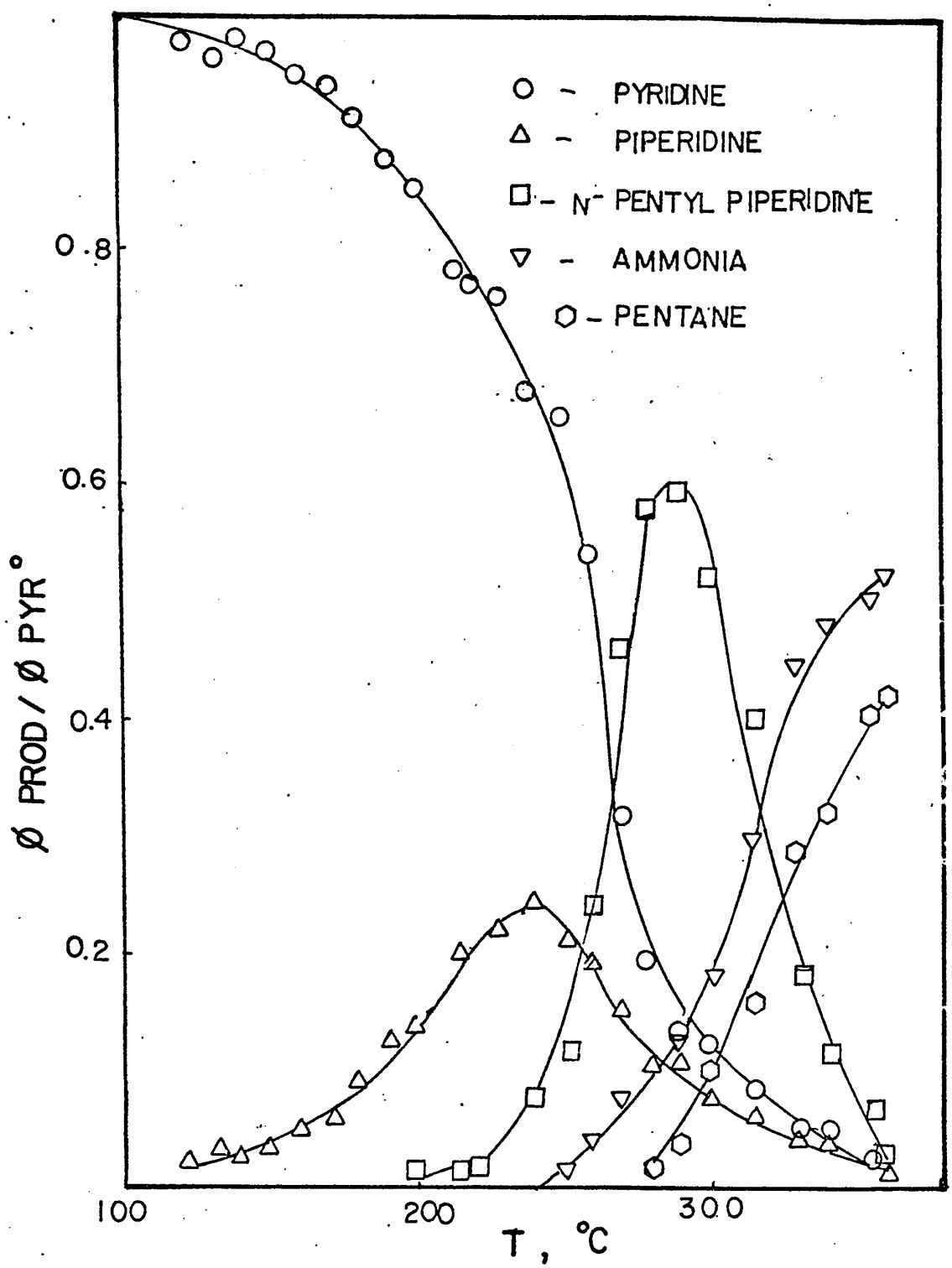

Fig. 5 The effect of temperature on product distribution at $\bar{R}$ = 29 .

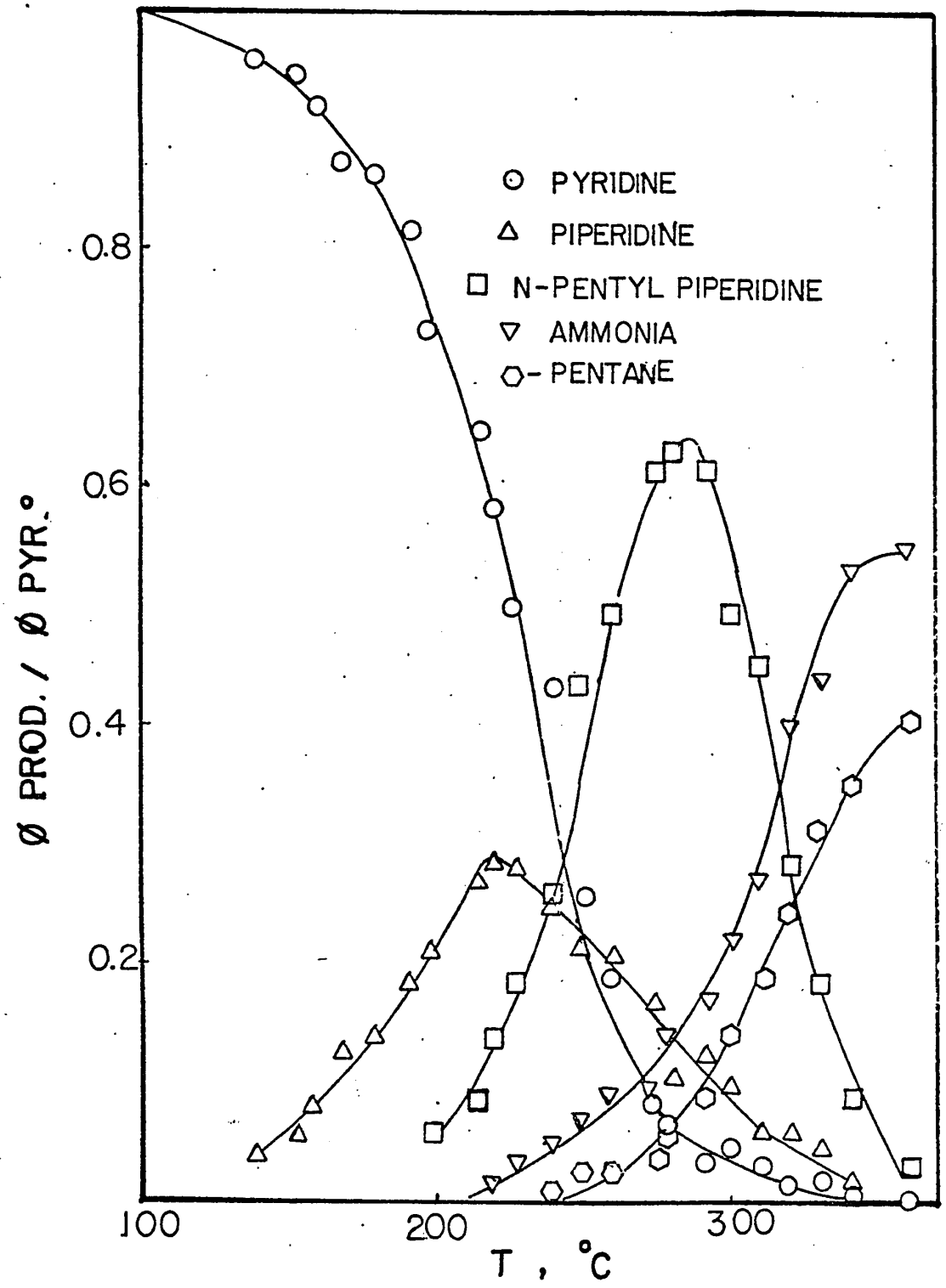

Fig. 6 The effect of temperature on product distribution at $\bar{R} = 40$.

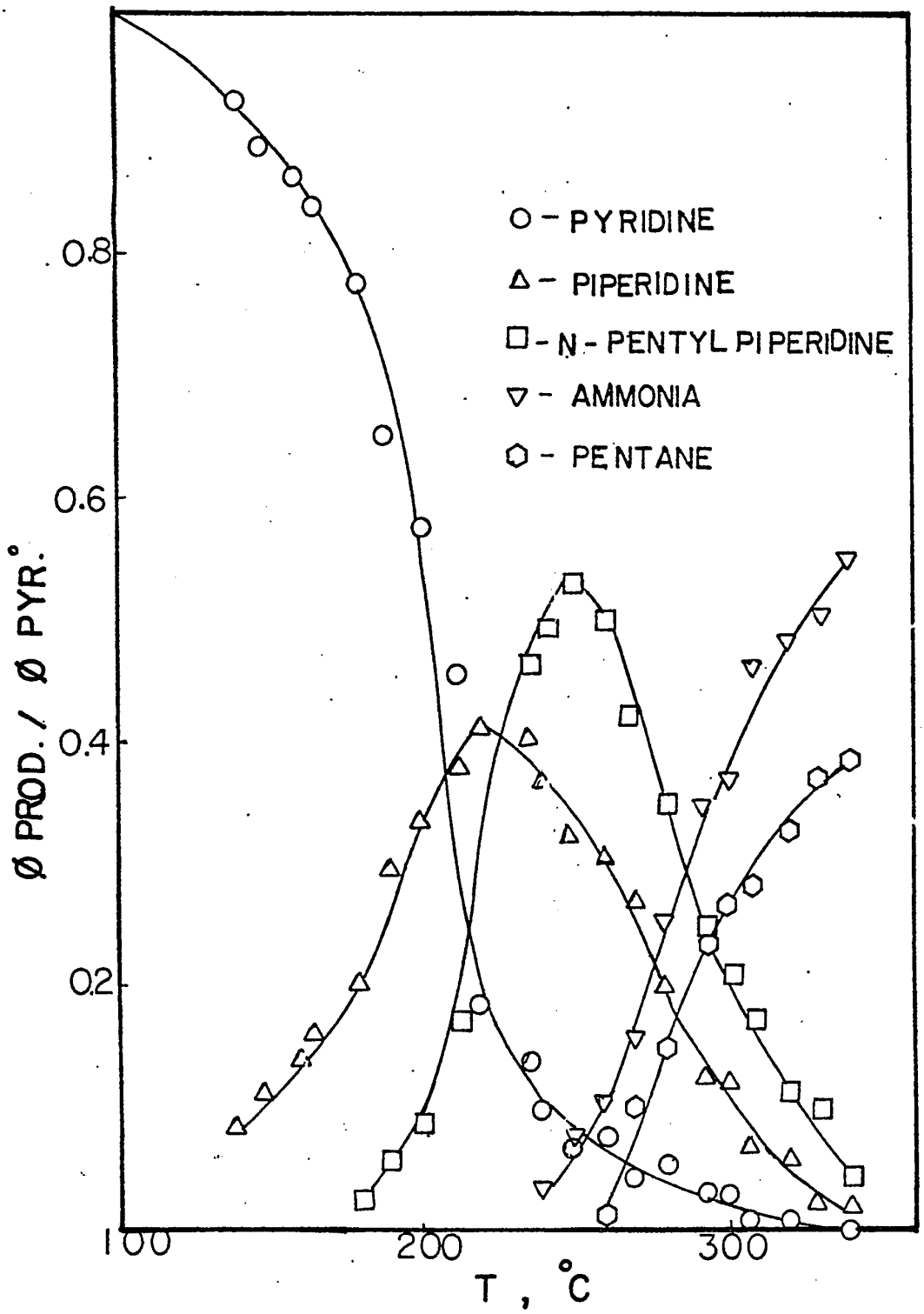

Fig. 7 The effect of temperature on product distribution at $\bar{R}$ = 60

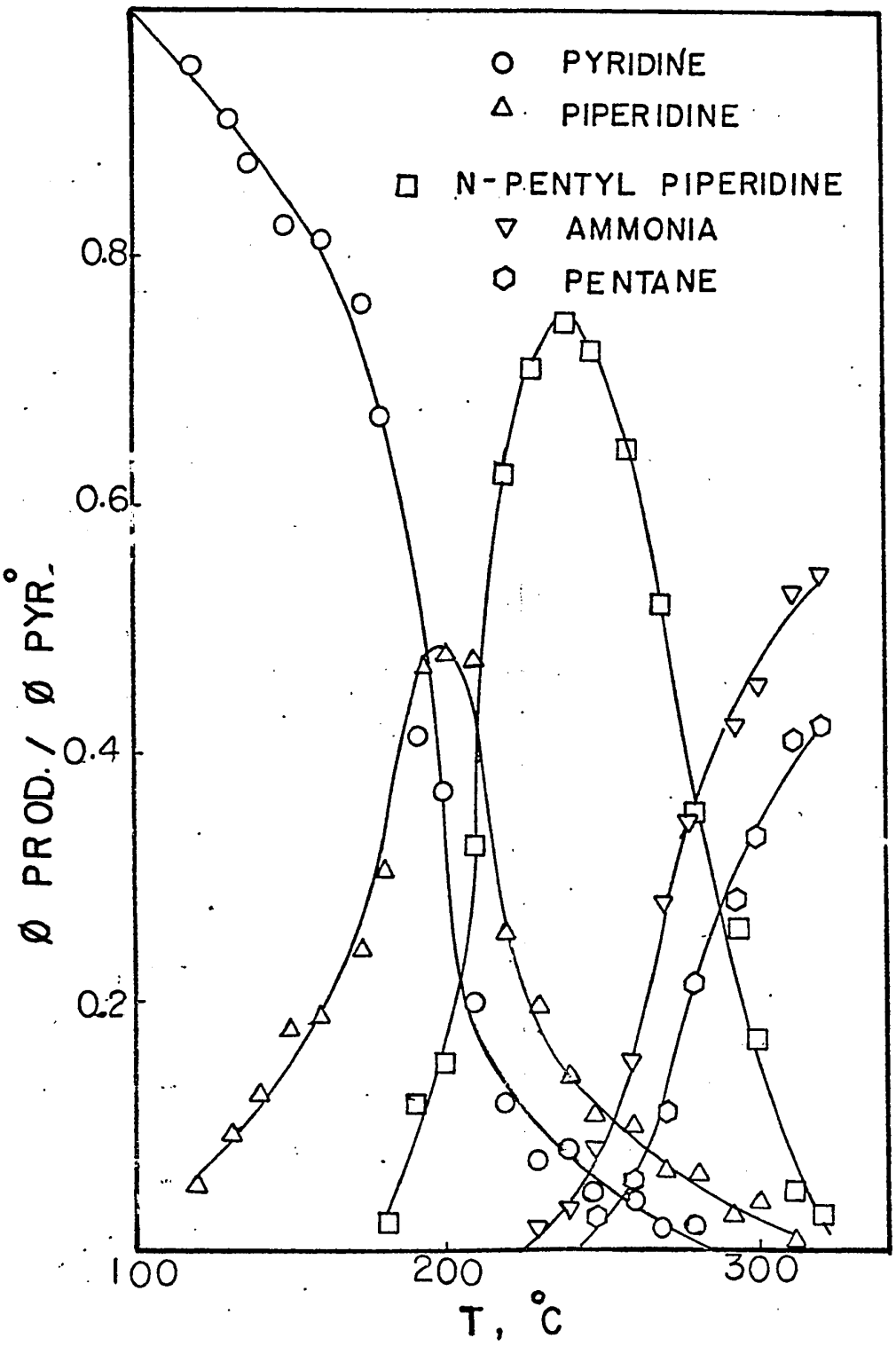

Fig. 8 The effect of temperature on product distribution at $\bar{R} = 80$

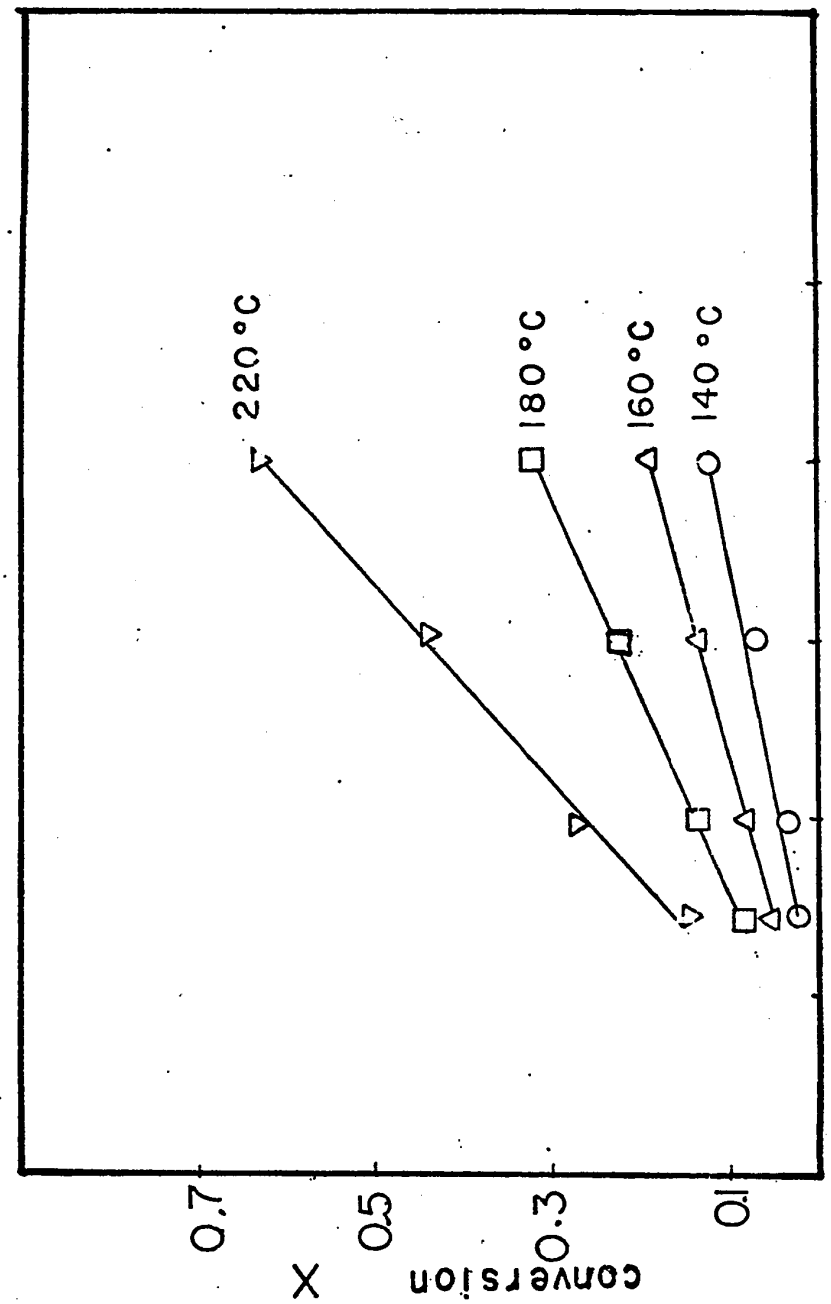

Fig. 9 The effect of mole ratio on conversin of pyridine

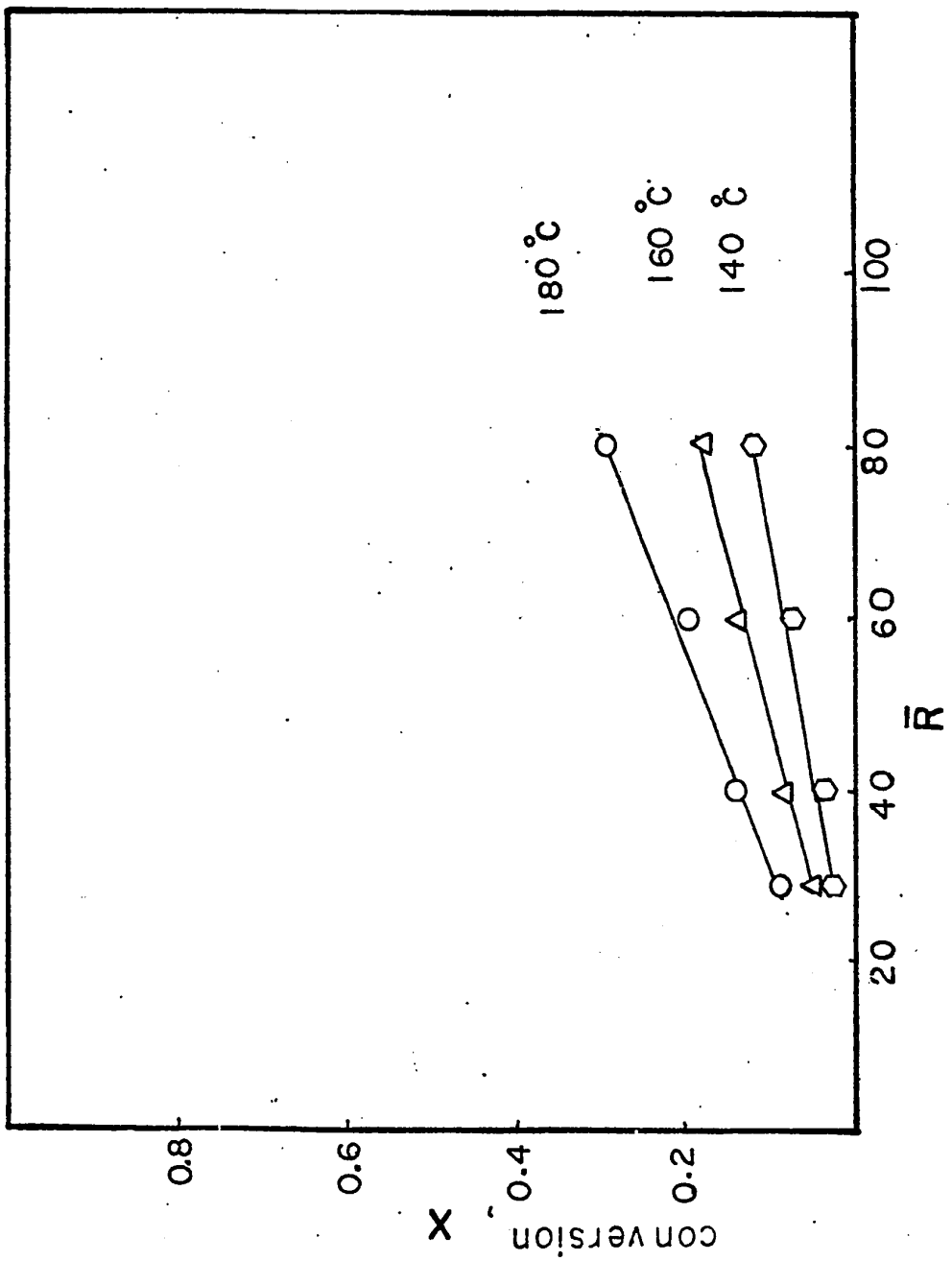

Fig. 10 The effect of mole ratio on conversion to piperidine

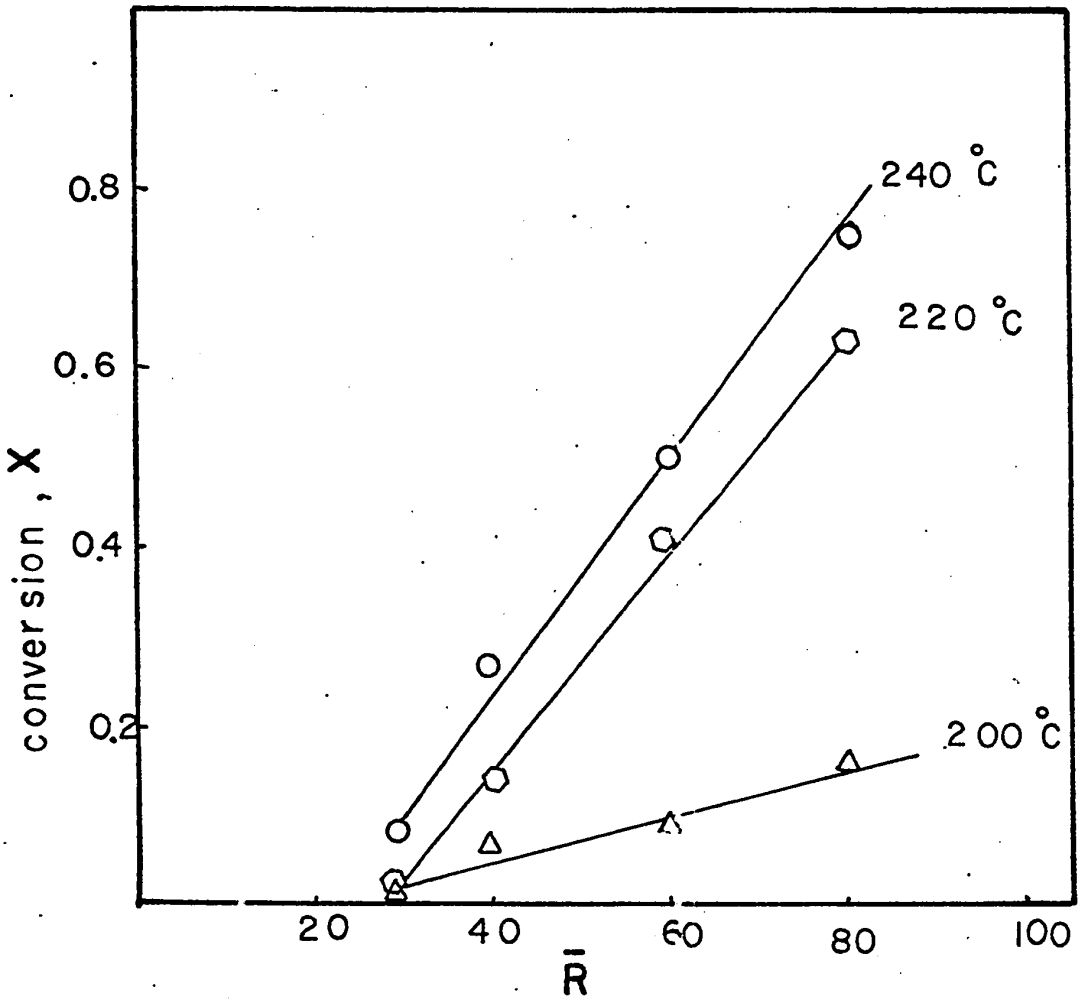

Fig. 11 The effect of mole ratio on conversion to n-pentyl piperidine.

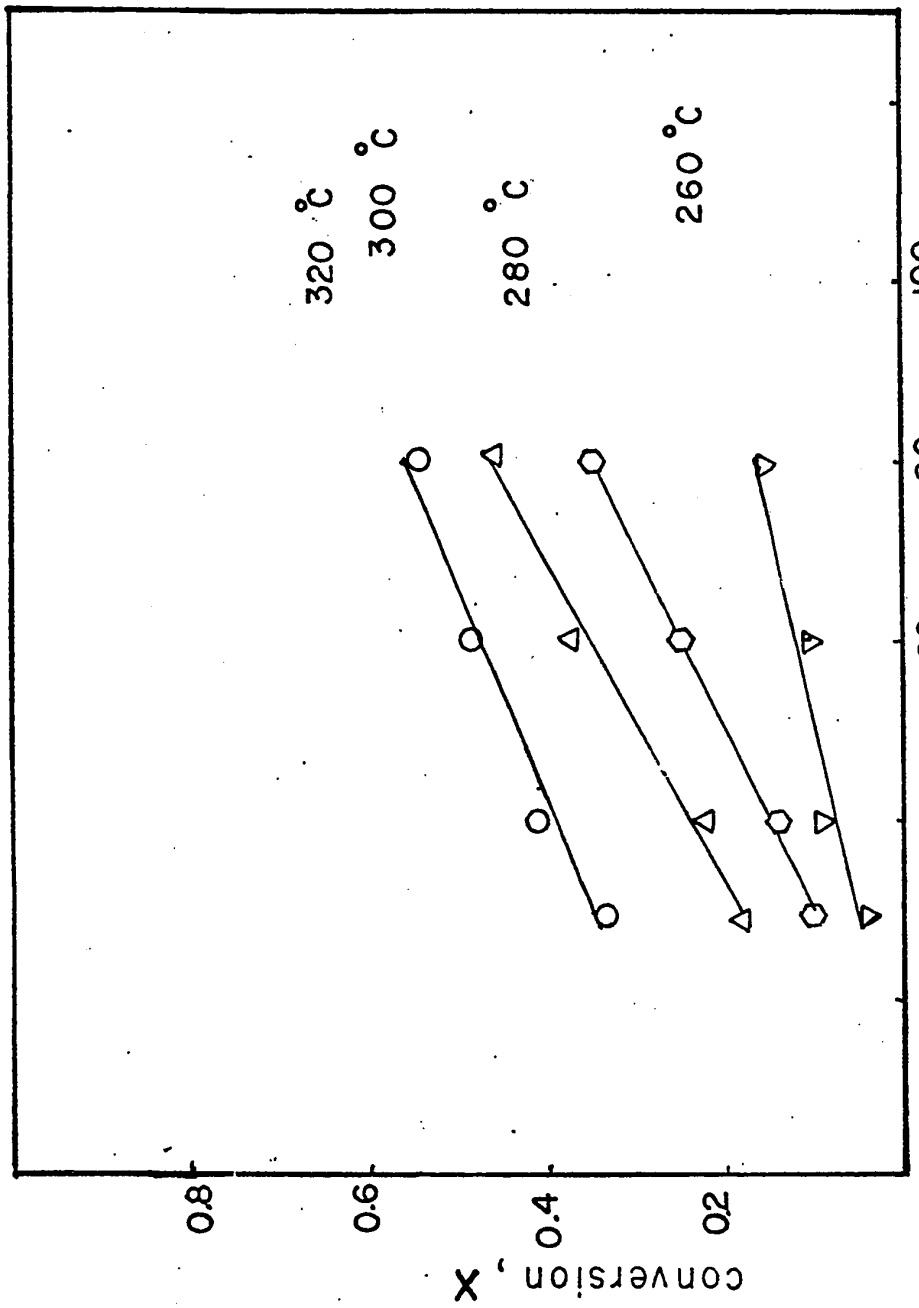

Fig. 12 The effect of mole ratio on conversion to ammonia

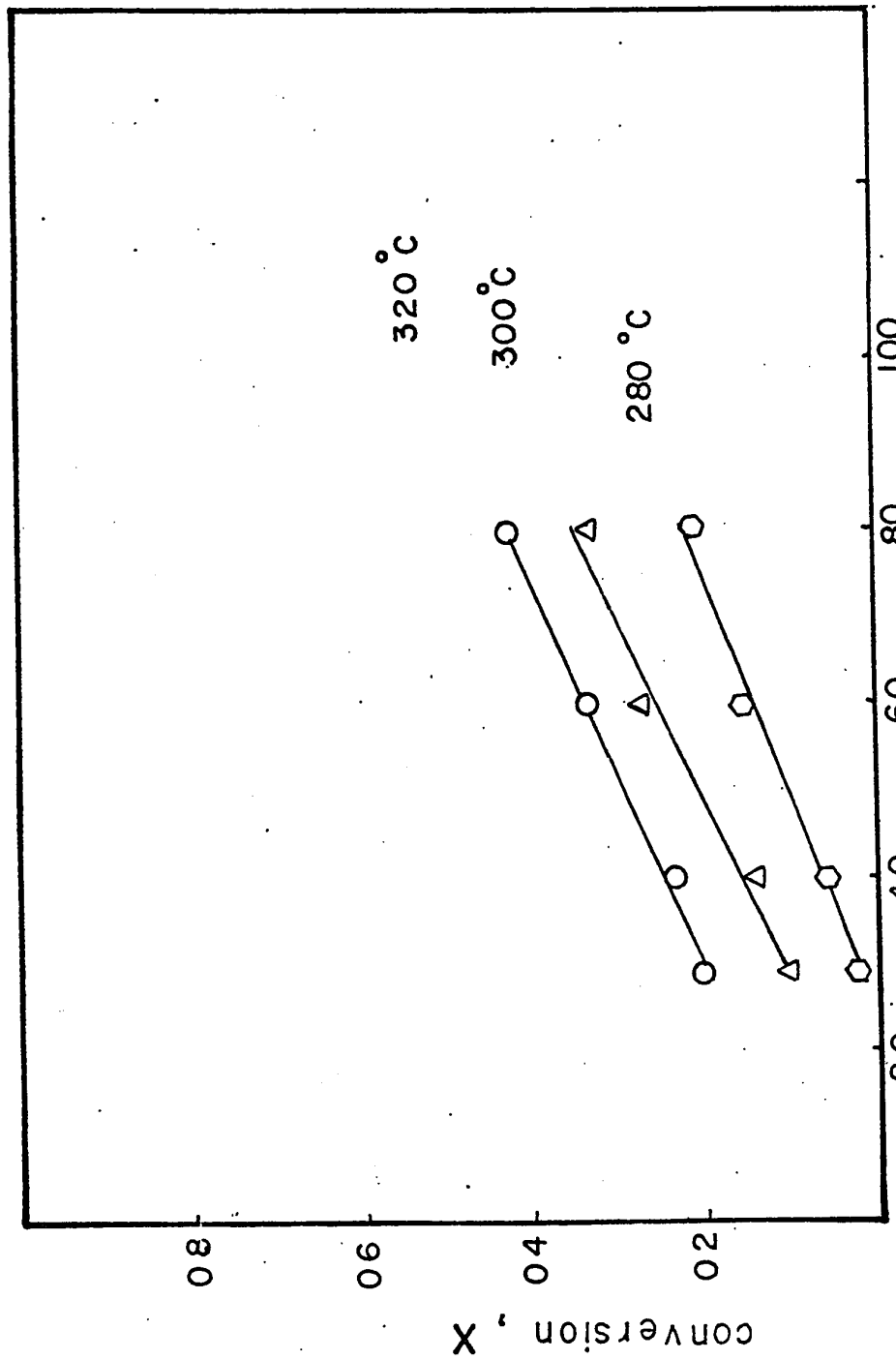

Fig. 13 The effect of mole ratio on conversion to pentane

The experimental data is presented in Tables 10-13. Plots of conversion (X) against W/F ratios at 145 and 195°C at $\overline{R}$ = 40, 50, 60 and 90 are shown in Figures 14 and 15. A linear relationship is noticed at these temperatures.

The plots of conversion (X) against W/F ratios at 245 and 280°C at $\overline{R}$ = 40, 50, 60 and 90 are shown in Figures 16 and 17.

The slopes were calculated at different W/F ratios from Figures 14-17. The slope at each W/F ratio was the experimental rate of reaction. By using a trial and error procedure, the experimental data were found to fit a rate equation of the form:

$$r = -\left[P_{py}^{\circ}\right] \frac{dX}{dt} = k_{ov} \left[P_{py}\right] \left[P_{H_2}\right]$$

The hydrogenation of pyridine was considered mainly:

$$\text{pyridine} + 3H_2 \xrightarrow{k_{ov}} \text{piperidine}$$

An integration of the above equation gives

$$\ln \frac{(\overline{R} - 3X)}{\overline{R}\ (1-X)} = k_{ov} \left[P_{py}^{\circ}\right] (\overline{R} - 3)\ t$$

The calculated data of the integrated expression at 145, 195, 245 and 280°C at $\overline{R}$ = 40, 50, 60 and 90 are given in Tables 14-17.

The values of the apparent rate constants at 145, 195, 245 and 280°C are tabulated in Table 18. By using a trial and error procedure, the values of the rate constants were found inversely proportional to the initial partial pressure of pyridine. Figure 22 shows a plot of k_{ov} against

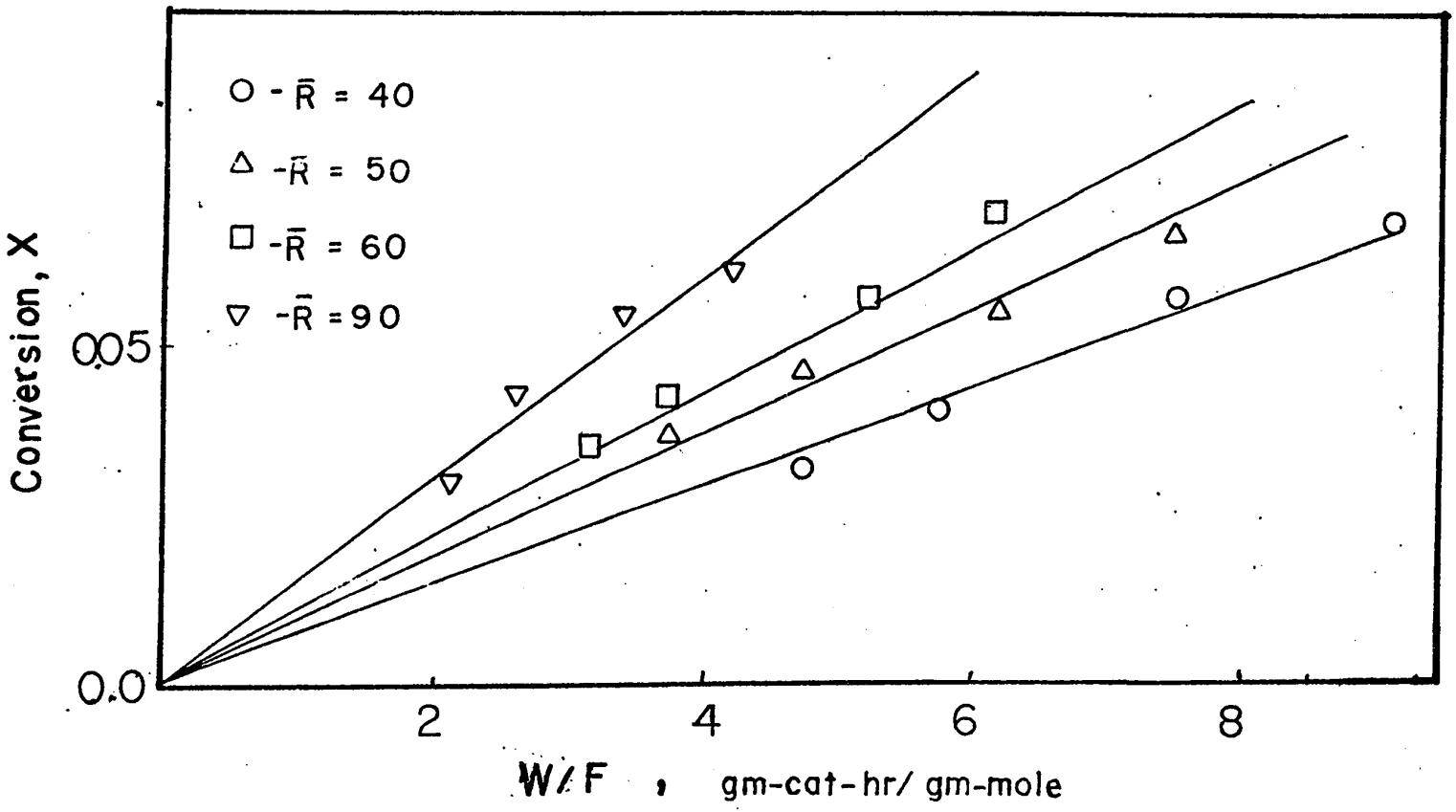

Fig. 14 The effect of residence time on conversion of pyridine at 145 °C

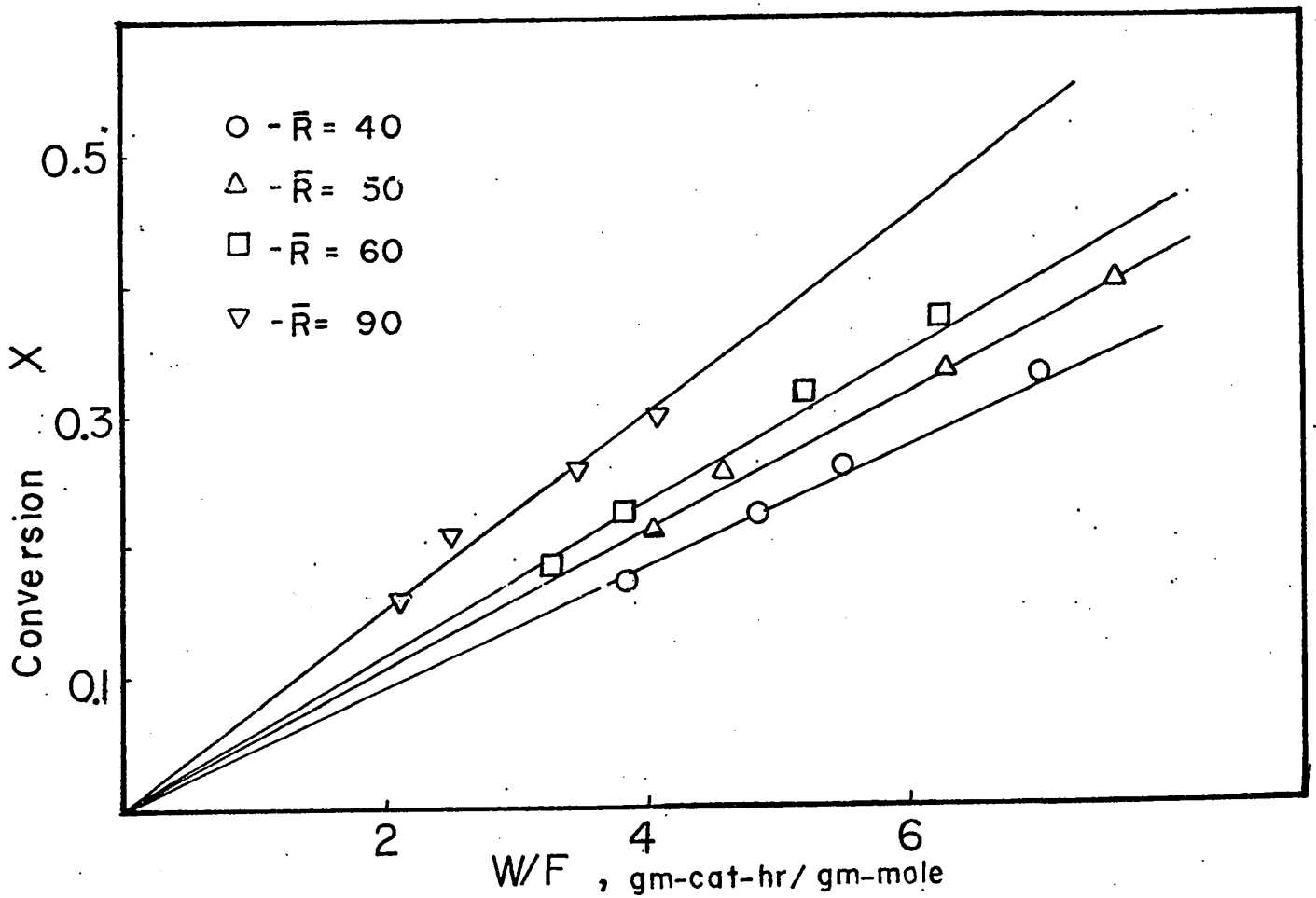

Fig. 15 The effect of residence time on conversion of pyridine at 195 °C

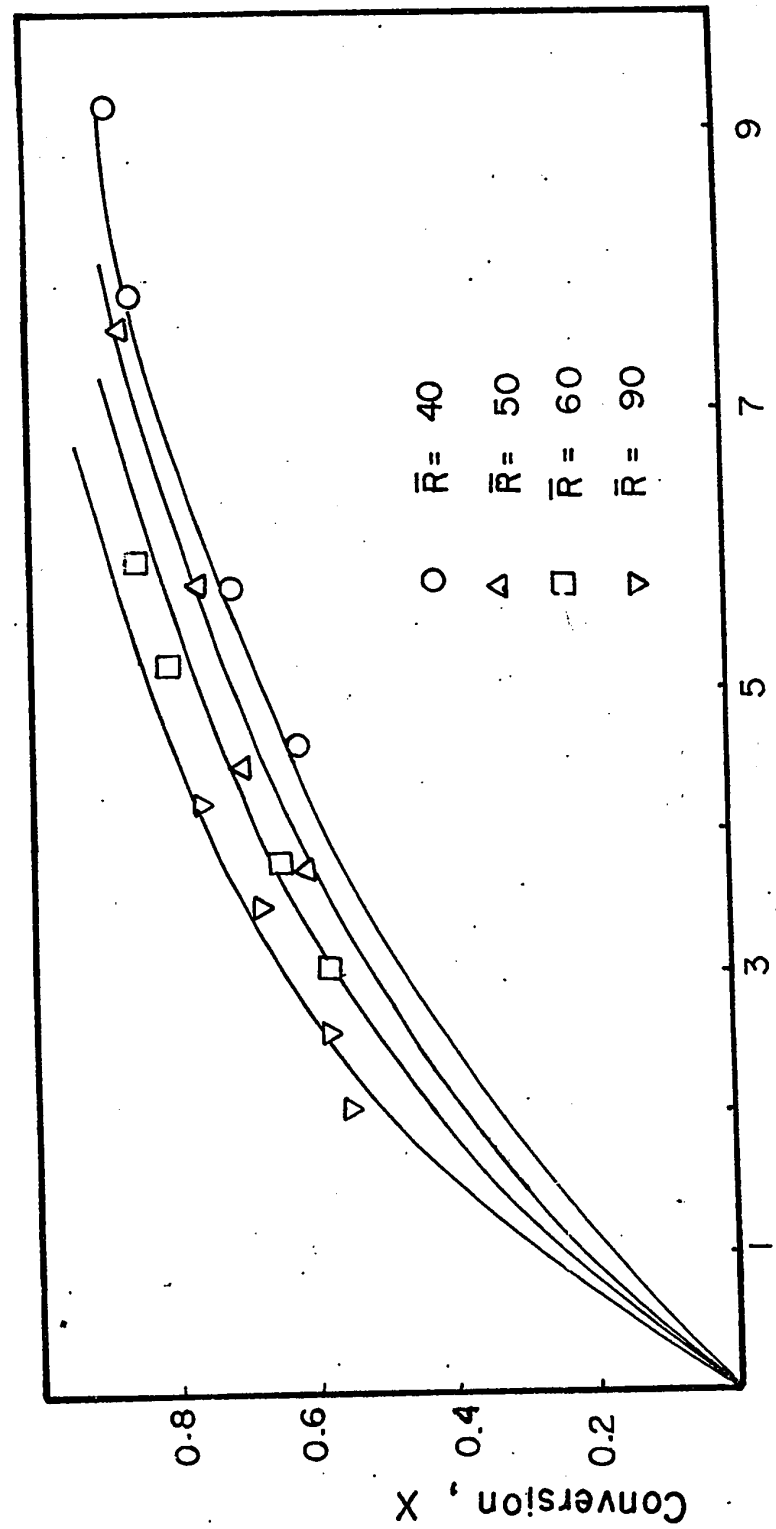

Fig. 16 The effect of residence time on conversion of pyridine at 245 °C

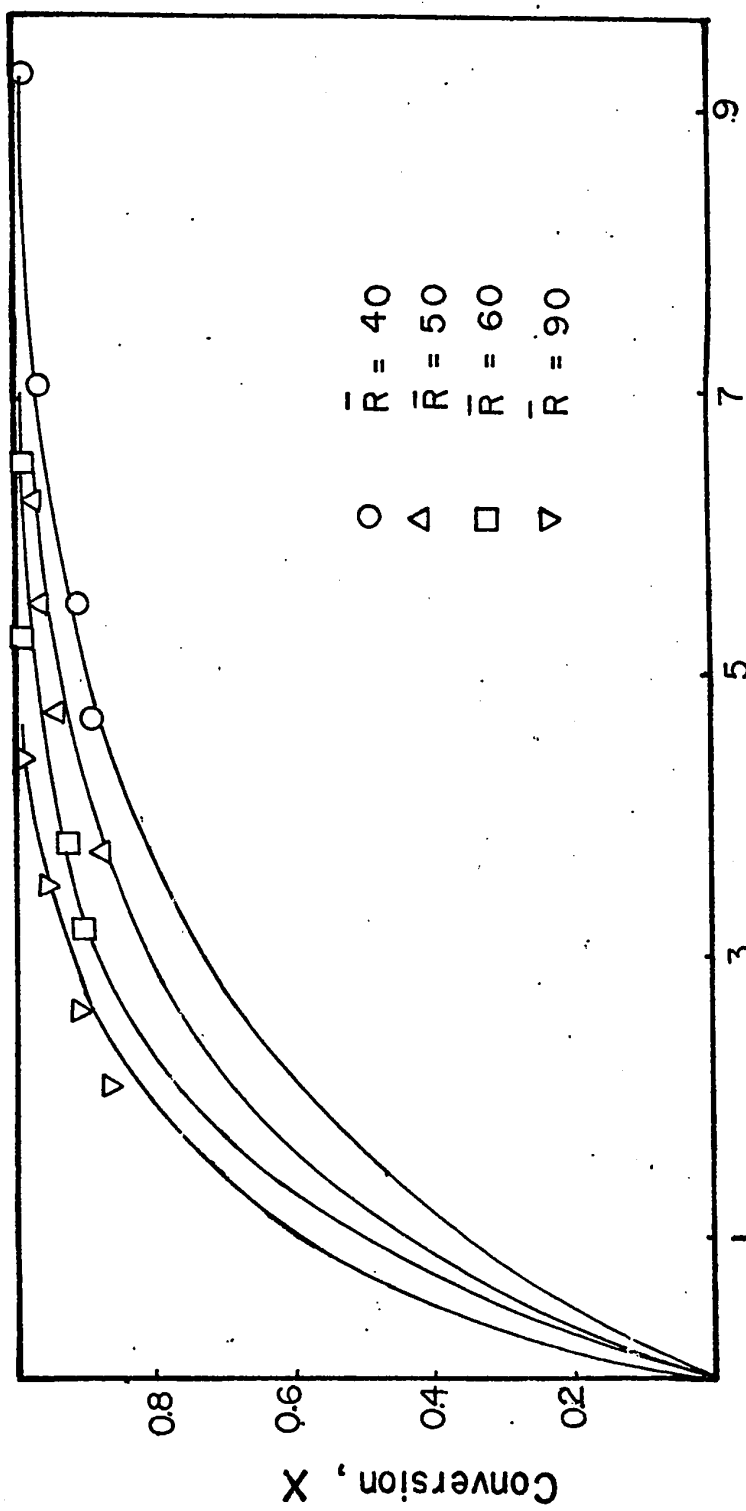

Fig. 17 The effect of residence time on conversion of pyridine at 280 °C

$1/\left[P_{py}^{\circ}\right]$. The rate constant was assumed to take the following form:

$$k_{ov} = k_s/\left[P_{py}^{\circ}\right] + k_i$$

The values of k_s and k_i are tabulated in Table 20 at 145, 195, 245 and 280°C.

The effect of temperature on the overall rate constant was studied to calculate the activation energy. A plot of log k_{ov} against 1/T at a constant mole ratio (Fig. 23) gave a straight line over a temperature range 145 to 280°C. While the activation energy was obtained from the slope the frequency factor was evaluated from the intercept of the plot.

A summary of results at hydrogen/pyridine ratios of 40, 50, 60 and 90 is given in Table 21.

IV-A Interpretation of results

The product distribution curves show that the hydrodenitrogenation of pyridine involve an intermediate. The reaction is believed to take the following scheme:

$$\text{pyridine} \xrightarrow[+3H_2]{k_{ov}} \text{piperidine} \xrightarrow[+H_2]{+pip} \text{n-pentylpiperidine} \xrightarrow[-pip]{+H_2} \text{ammonia + pentane}$$

The experimental rates were obtained by determining the slopes at various W/F rations from X vs W/F curves. Different rate equations were tried to fit the experimental data. The rate equations suggested in the literature (16, 14) made the choice easier. A rate equation of the form:

$$r = -\left[P_{py}^{\circ}\right] \frac{dX}{dt} = k_{ov} \left[P_{py}\right] \left[P_{H_2}\right]$$

was found to fit the experimental data closely. This rate equation was used to evaluate the rate constant by using the integral method. The rate of the chemical reaction:

$$\text{pyridine} + 3H_2 \xrightarrow{k_{ov}} \text{products}$$

can be written as:

$$r = -\left[P_{py}^{\circ}\right] \frac{dX}{dt} = k_{ov}\left[P_{py}^{\circ}\right]^2 (1-X)(\bar{R} - 3X)$$

where X = conversion of pyridine

$\bar{R}$ = mole ratio (H_2/pyridine).

$\left[P_{py}^{\circ}\right]$ = Initial partial pressure of pyridine.

k_{ov} = overall rate constant.

$$-\frac{dX}{(1-X)(\bar{R}-3X)} = k_{ov}\left[P_{py}^{\circ}\right] dt$$

By integrating the above expression we get

$$\log \frac{(\bar{R} - 3X)}{\bar{R}(1-X)} = k_{ov}\left[P_{py}^{\circ}\right](\bar{R} - 3)\, t$$

A plot of $\log \frac{(\bar{R} - 3X)}{\bar{R}(1-X)}$ against t or W/F gave a straight line with a slope of $k_{ov}\left[P_{py}^{\circ}\right](\bar{R} - 3)$.

The rate constants calculated from the relationship:

$$k_{ov} = \text{slope} / \left[P_{py}^{\circ}\right](\bar{R} - 3)$$

should be dependent on temperature only. However k_{ov} calculated was found to be dependent on the pyridine concentration of the feed stream. A plot of k_{ov} against $1/\left[P_{py}^{\circ}\right]$ resulted in a straight line which suggested that the pseudo-rate constant k_{ov} can be defined as:

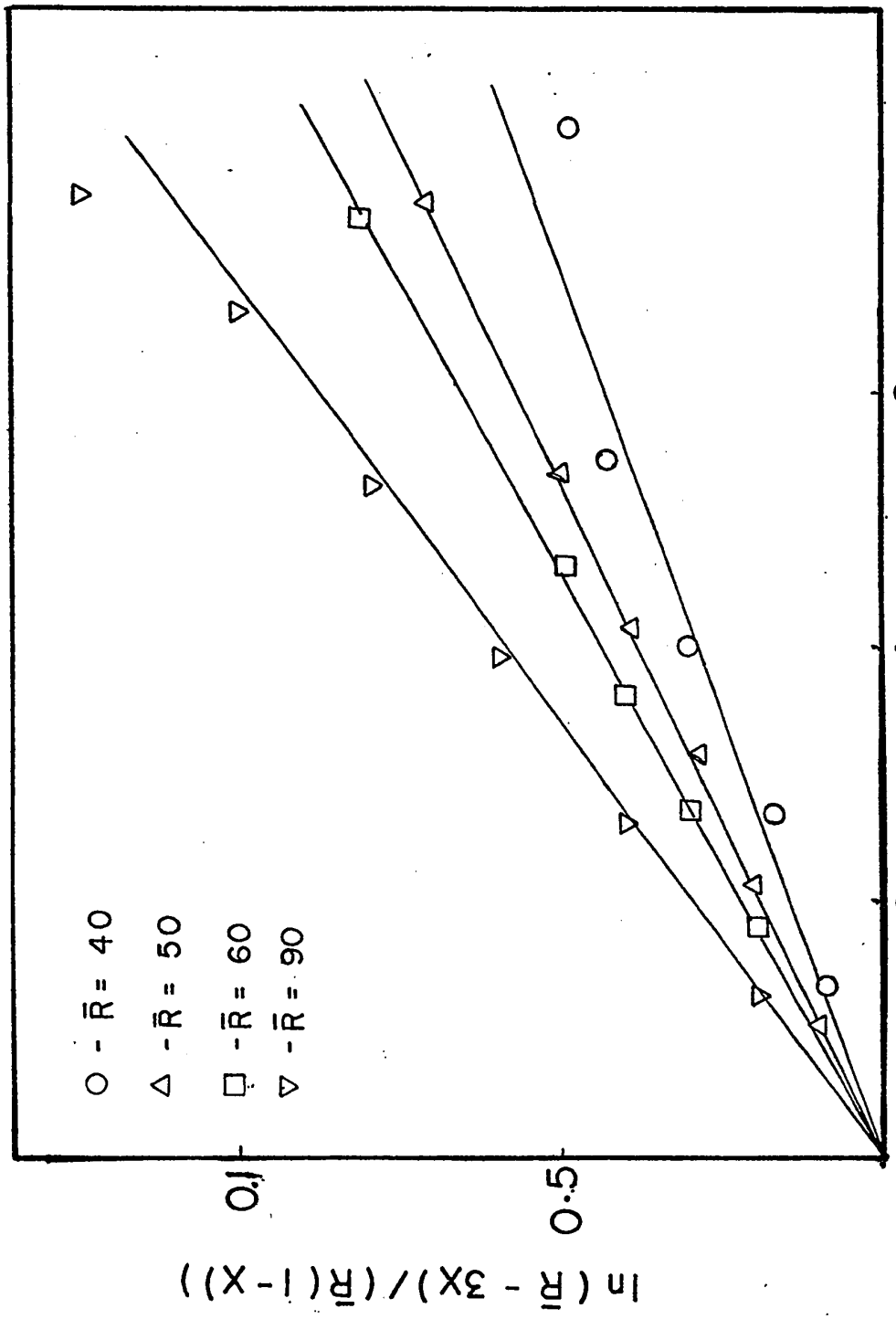

Fig. 18 Calculation of k_{ov} at 145 °C

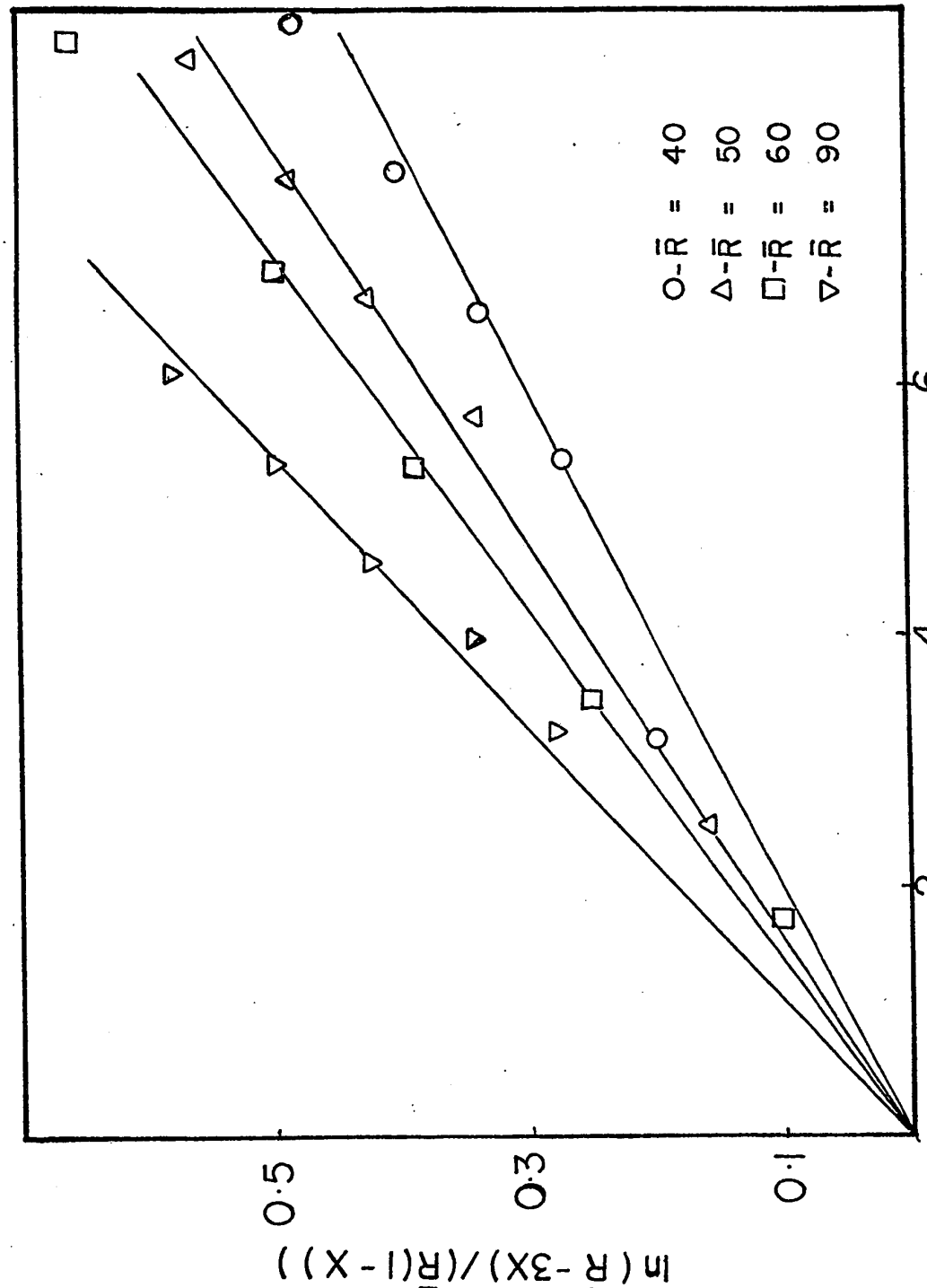

Fig. 19 Calculation of k_{ov} at 195 °C

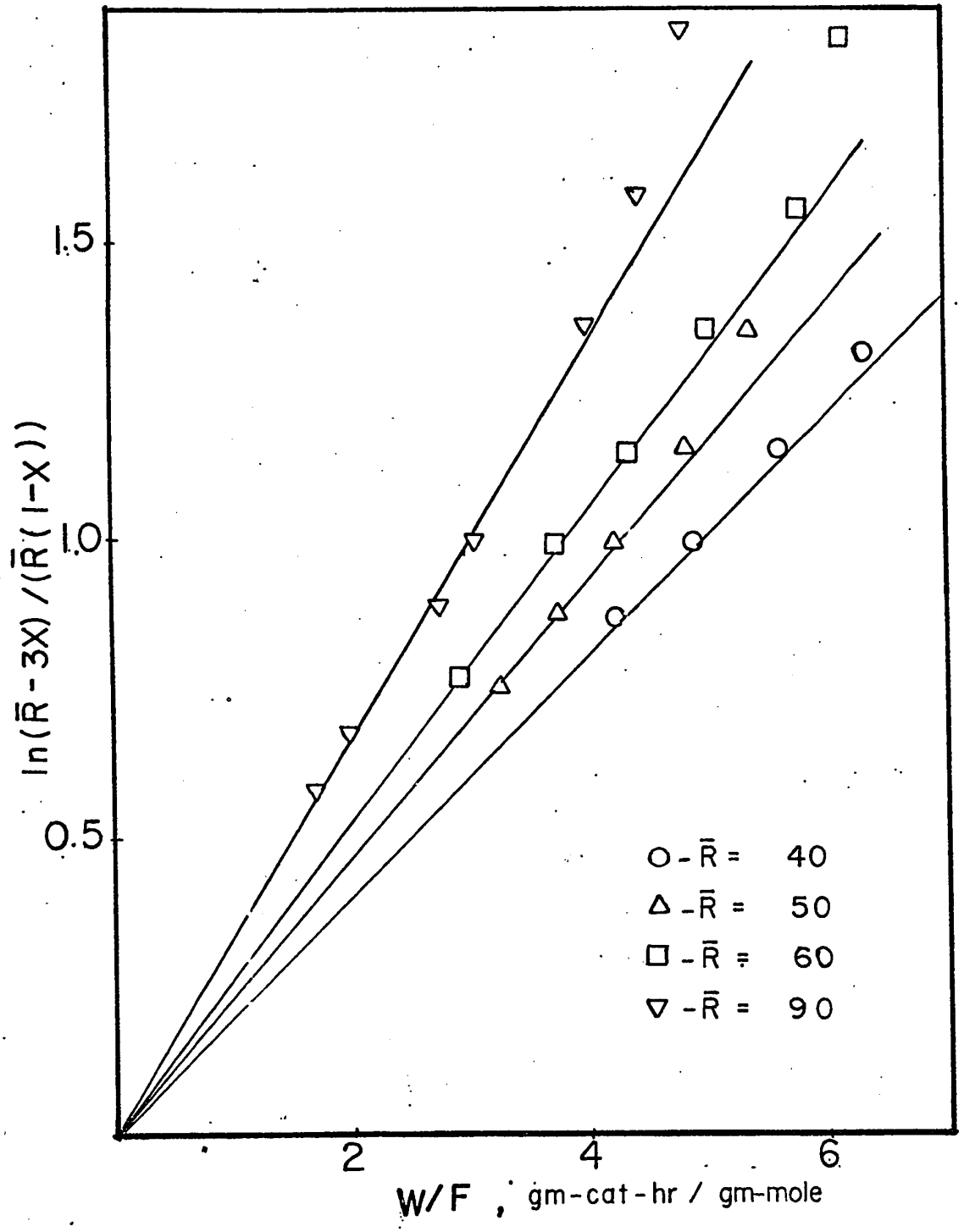

Fig. 20 Calculation of k_{ov} at 245 °C

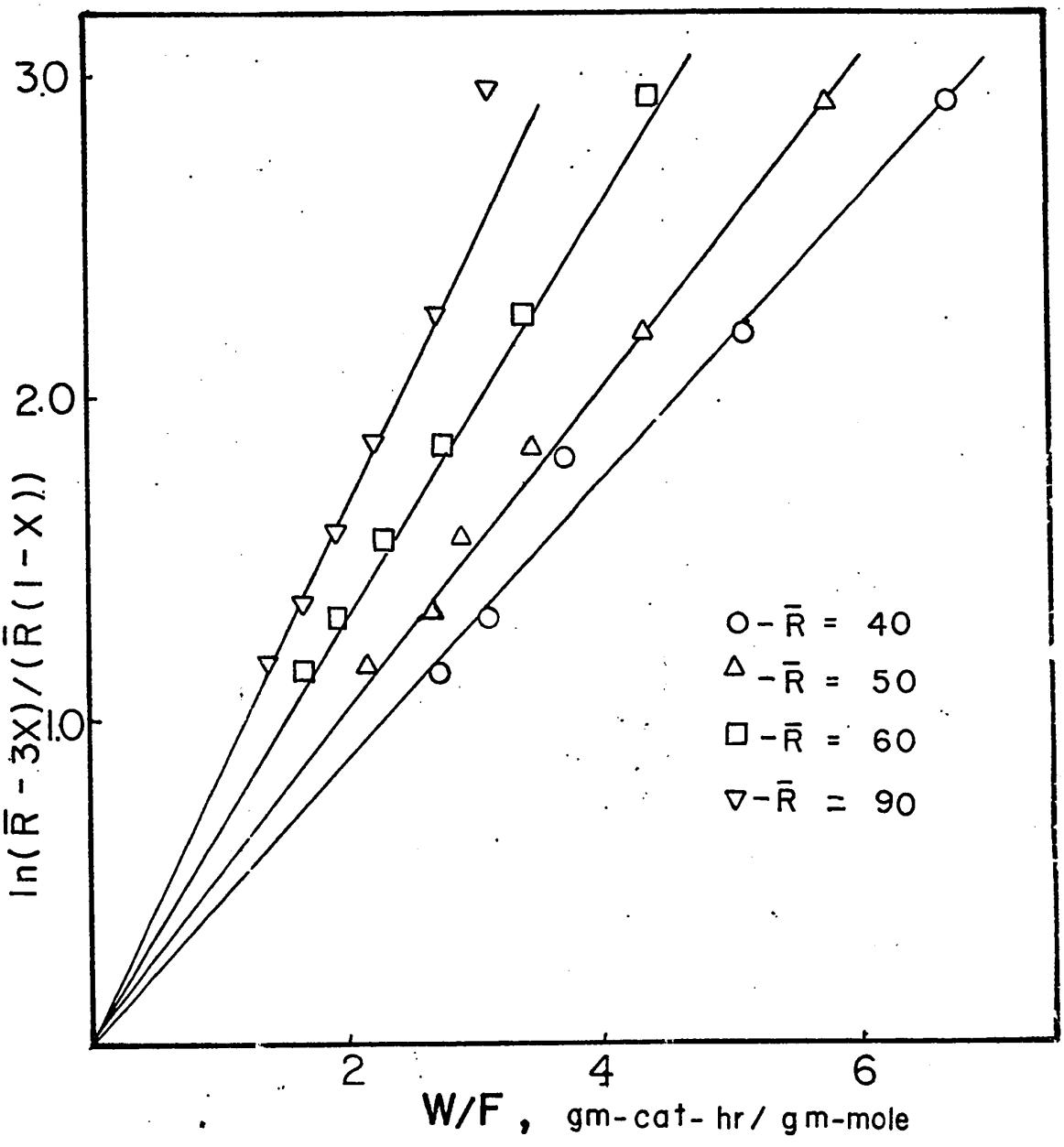

Fig. 21 Calculation of k_{ov} at 280°C

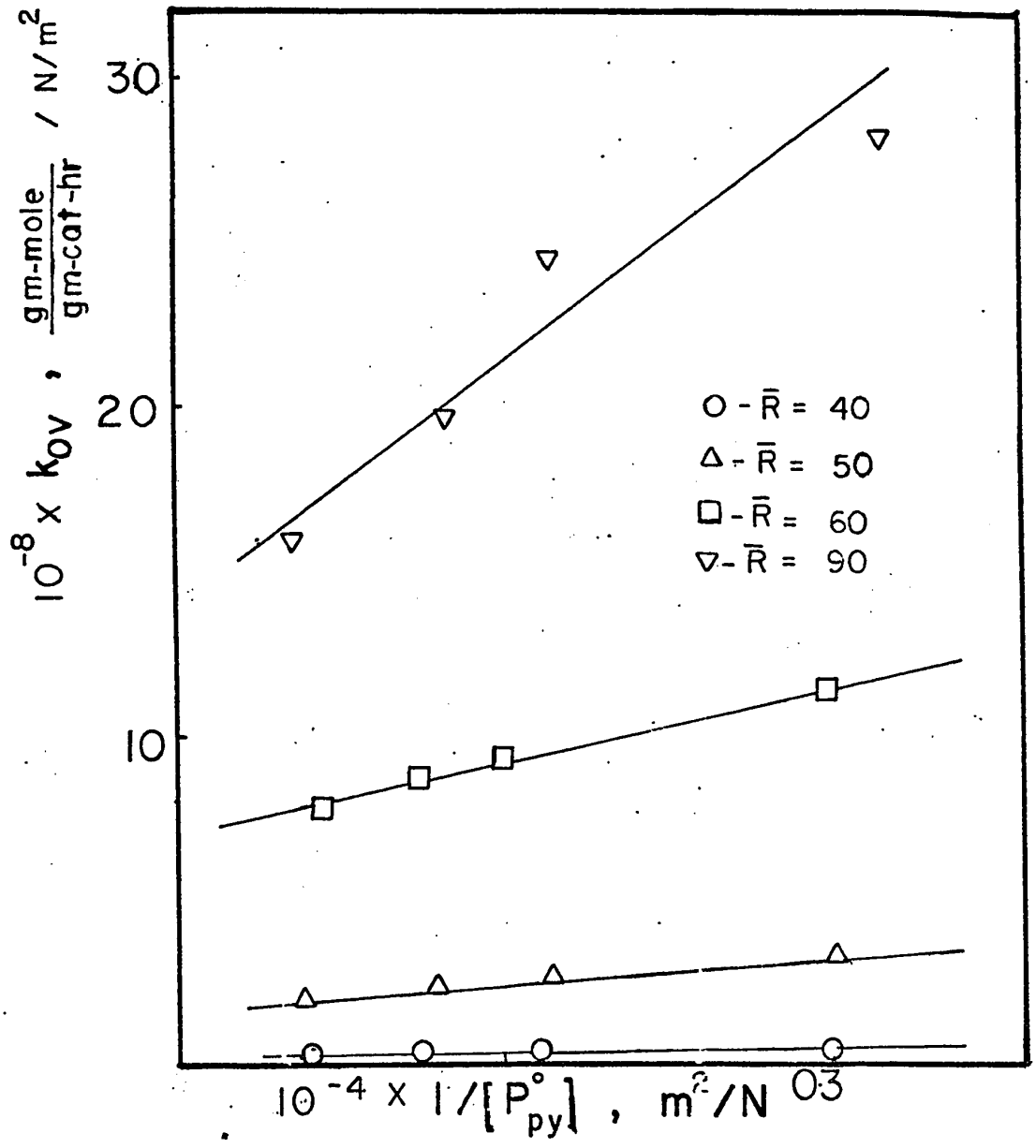

Fig. 22 The effect of initial partial pressure of pyridine on k_{ov}.

$$k_{ov} = k_s / \left[P_{py}^{\circ}\right] + k_i$$

$$\bar{R} = \left[P_{H_2}^{\circ}\right] / \left[P_{py}^{\circ}\right]$$

$$\text{or} \quad k_{ov} = k_s \frac{\bar{R}}{\left[P_{H_2}^{\circ}\right]} + k_i$$

k_s and k_i were calculated from k_{ov} against $1/\left[P_{py}^{\circ}\right]$ plot at temperatures of 145, 195, 245 and 280°C.

The rate equation thus evaluated is expressed as:

$$r = -\left[P_{py}^{\circ}\right] \frac{dX}{dt} = \left(k_i + k_s \frac{\bar{R}}{\left[P_{H_2}^{\circ}\right]}\right)\left[P_{py}\right]\left[P_{H_2}\right]$$

This is first order with respect to both pyridine and hydrogen concentrations.

The overall rate constant (k_{ov}) was assumed to be constant at a constant mole ratio. A plot of log k_{ov} vs 1/T, where T in °K, gave a straight line (Figure 23). The activation energy was obtained from the slope of the line according to the equation:

$$k_{ov} = k_o \exp\left(-Ea / RT\right)$$

$$\log k_{ov} = \log k_o - \frac{Ea}{R} \cdot \left[\frac{1}{T}\right]$$

Such plots were made for the mole ratios 40, 50, 60 and 90. The activation energies calculated at the above mole ratios showed consistency. The values of activation energies and frequency factors at various mole ratios of hydrogen/pyridine are given in Table 20.

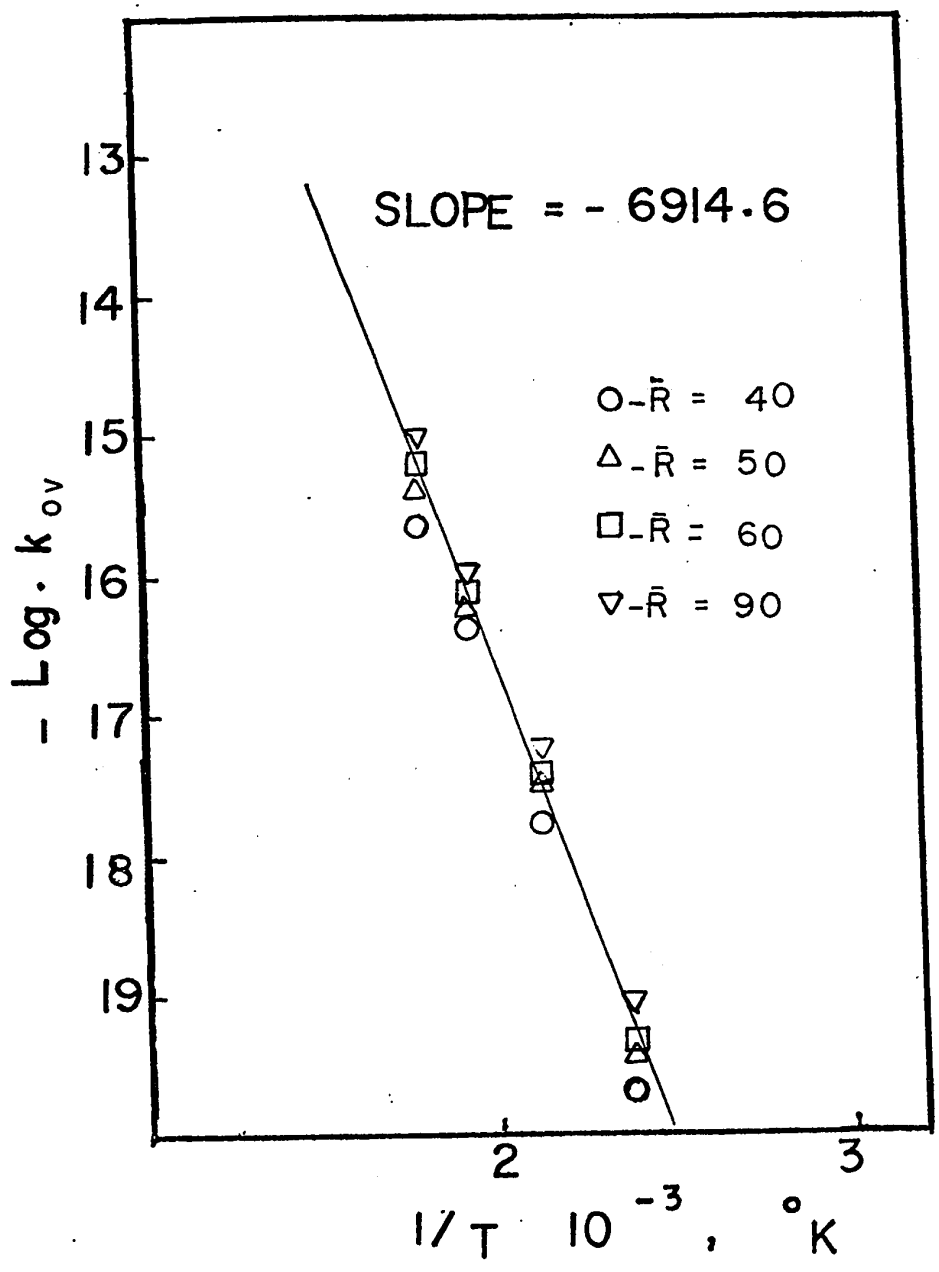

Fig. 23 The effect of temperature on k_{ov}

V. KINETIC ANALYSIS OF DATA

V-A Steps of a Heterogeneous Reaction

In order to understand the reaction rate, it is necessary to understand the theoretical background and the assumptions that are used to derive a rate expression. Smith (26) has suggested that a hetrogeneous reaction (gas-solid) takes place according to the following steps:

1. Transport of reactants from the bulk fluid to the fluid-solid interphase. (External surface of catalyst particle.)
2. Intraparticle transport of reactants into the catalyst particle. (Porous catalyst)
3. Adsorption of reactants at interior sites of the catalyst particle.
4. Chemical reaction of adsorbed reactants to adsorbed products. (Surface reaction)
5. Desorption of adsorbed products.
6. Transport of products from interior sites to the outer surface of the catalyst particle.
7. Transport of products from the fluid-solid interface into the bulk fluid stream.

For a non porous catalyst diffusion inside the pores can be assumed to be negligible and thus steps (2) and (6) can be eliminated. Also if the bulk flow is assumed turbulent (high velocity of reactants past the solid particles) then steps (1) and (7) can be eliminated, and the reaction then takes place through steps (3), (4) and (5).

V-B Factors Affecting the Rate Mechanism

In kinetic studies dealing with gaseous reaction catalyzed by solid catalyst, there are many factors which might lead to an error in the interpretation of the reaction model if they are not considered. These factors can be summarized as follows:

1. Negligence of external resistance of mass and heat transfer.
2. Negligence of internal diffusion.
3. Departure from plug flow.
4. Homogeneous reactions catalyzed by the reactor wall.
5. Catalyst activity and deactivation.

(1) External Resistance of Mass and Heat Transfer

In this experiment the temperature and the partial pressure at the catalyst site is assumed equal to those of the ambient stream. This can simplify the correlation of experimental data and the reaction rate. The following is a derivation of how important is the effect of mass and heat transfer on these assumptions.

The general equation mass transfer and heat transfer are given as:

$$r_{mA} = K_G a_m \phi (P_A - P_{Ai}) \qquad \text{I}$$

$$r_h = -h_G a_m \phi (T - T_i) \qquad \text{II}$$

where

r_{mA} = rate of reaction or mass transfer of A per unit mass of catalyst.

r_h = heat transfer due to heat of reaction per unit mass of catalyst.

K_G = mass transfer coefficient for component A.

h_G = heat transfer coefficient for component A.

P_A = partial pressure of component A in the ambient stream.

P_{Ai} = partial pressure of component A at the catalyst surface.

T = temperature of the ambient stream.

T_i = temperature of the catalyst.

a_m = external surface area of catalyst per unit mass.

ϕ = shape factor of the catalyst particles, equal to 0.1 for spheres, 0.9 for irregular particles.

$\frac{D_p G}{\mu}$ is modified Reynold's number.

G = mass velocity of flow based on the total cross-sectional area of the bed, mass per unit time per unit area.

D_p = effective particle diameter = $\frac{a_p}{\pi}$.

π = total pressure.

a_p = average surface area per particle.

Gamson, Thodes, Wilke and Hougan in a series of articles developed expressions for J_h and J_d for the range of Reynold number above 350, for $\frac{D_p G}{\mu} > 350$

$$J_d = 1.82 \left(\frac{D_p G}{\mu}\right)^{-0.51} \qquad \text{III}$$

$$J_h = 1.95 \left(\frac{D_p G}{\mu}\right)^{-0.51} \qquad \text{IV}$$

for $\frac{D_p G}{\mu} < 350$

$$J_d = 0.09 \left(\frac{D_p G}{\mu}\right)^{-0.41} \qquad \text{V}$$

$$J_h = 1.06 \left(\frac{D_p G}{\mu}\right)^{-0.41} \qquad \text{VI}$$

Experimental data on mass transfer are related to K_G by the relationship

$$J_d = \left(\frac{K_G M_m P_{fA}}{G}\right) \left(\frac{\mu}{\rho D_{AM}}\right)_f^{2/3} \qquad \text{VII}$$

Experimental data on heat transfer are related to h_G by the relationship,

$$J_h = \left(\frac{h_G}{C_p G_m}\right) \left(\frac{C_p \mu}{k}\right)_f^{2/3} \qquad \text{VIII}$$

where,

$\left(\frac{\mu}{\rho D_{AM}}\right)$ = dimensionless schmidt number

$\left(\frac{C_p \mu}{k}\right)$ = dimensionless prandtl number

D_{AM} = Average diffusion coefficient of component A.

C_p = Specific heat of the gas.

G_m = mass velocity of the gas flowing based upon the total cross-sectional area of the bed.

k = thermal conductivity of the gas.

μ = viscosity of the gas.

ρ = density of the gas.

P_{fA} = film pressure factor, defined by equation IX.

M_m = mean molecular weight

The film pressure factor in equation (VIII), was defined as follows:

for a reaction

$$aA + bB = rR + sS$$

$$P_{fA} = \frac{(\pi + \delta_A P_A) - (\pi + \delta_A P_{Ai})}{\ln \frac{(\pi + \delta_A P_A)}{\pi + \delta_A P_{Ai}}} \qquad \text{IX}$$

where

$$\delta_A = \frac{r + s + a + b}{a}$$

if $(\pi + \delta_A P_A) / (\pi + \delta_A P_{Ai})$ is less than 1.2, the arithmatic mean is sufficiently accurate for practical purposes. Yoshida et al. (28) describe a method to estimate the temperature and partial pressure at the surface of a catalyst particle for a gaseous reactions in a flow system.

$$\frac{\Delta P_A}{P_A} = \Delta Y_A = R\,(J_d)^{-1}\; Y_{fA}\,(Sc)^{2/3} \qquad \text{X}$$

$$\Delta T = Q\,(J_h)^{-1}\,(Pr)_f^{2/3} \qquad \text{XI}$$

$$Q = \frac{r_{mA}\,\Delta H_A}{a_m\,\phi C_p G_m} \qquad \text{XII}$$

ΔH_A = molal heat of reaction of component A

Pr = Prandtl number = $\frac{C_p \mu}{k}$

$$R = \frac{r_{mA}}{a_m\,\phi\,G_m}$$

Sc = schmidt number = $\frac{\mu}{\rho\,D_{AM}}$

$$Y_{fA} = \frac{P_{fA}}{\pi}$$

J values are calculated from the correlation with Reynolds number $\left(\frac{G}{a_v \phi \mu}\right)$ as follows:

if $0.01 < Re < 50$

$$J_d = 0.84\ Re^{-0.51} \qquad \text{XIII}$$

if $50 < Re < 1000$

$$J_d = 0.57\ Re^{-0.41} \qquad \text{XIV}$$

and

$$J_h = 0.076\ J_d \qquad \text{XV}$$

All terms in equation (XII) are dimensionless except ΔT and Q which have the dimension of temperature. Yoshida (28) concluded that while Q was the most significant term in controlling the temperature drop, R was the most significant in controlling the pressure drop. Experimental data relating $\Delta p_j/p_j$ to $R/_{yj}$ and ΔT to Q was prescribed.
Both Q and R are proportional to $r_A\ D_p^{n+1}\ G_m^{n-1}$ since n is a fraction, it is clear that by increasing the gas flow rate or decreasing the particle size the mass and heat transfer resistances can be eliminated.

A sample calculation based on the method of Yoshida et al. is shown in Appendix (B). The partial pressure gradient was found to be of the order 0.001 and temperature difference across the gas film was found to be less than 0.1°C. Hence these effects could be neglected.

(2) Internal Diffusion

As most of the catalysts are porous, their external surface area constitutes a small fraction of the total

surface area on which the reaction takes place. Most reactions occur on the inner surface of the porous structure. The diffusion of reactants into and the products out of them could be important factors in controlling reaction rate. Two types of diffusion in pores are possible - bulk or molecular diffusion, and Knudsen diffusion, depending on whether the mean free path between intermolecular collisions is small or large compared with the pore size. For most conditions the operation of catalytic reactors, the pore diffusion is of the Knudsen type. Molecular diffusion predominates only at high pressure or at atmospheric pressure with catalyst having very large pore (>5000°A radius). In this study, the effect of molecular diffusion was determined by varying the feed velocity of pyridine while keeping temperature, hydrogen/pyridine mole ratio and the particle size of the catalyst constant. Two runs were carried out at a temperature of 245°C, a hydrogen/pyridine mole ratio of 40, a catalyst diameter of 20-40 mesh size and residence time of 5.75 gm-cat-hr/gm-mole. The feed rates of pyridine in these two runs were 6.419×10^{-4} and 3.893×10^{-4} mole/min respectively. The experimental data is shown in Appendix D. The results showed that molecular diffusion did not control the reaction rate.

The effect of Knudsen diffusion is evaluated from the knowledge of effectiveness factor of the catalyst. This factor is defined as the ratio of the actual reaction rate per unit mass of the catalyst to the rate which would exist

if the concentration of all interior surfaces were the same as those of the gross exterior surface (30). Although much effort have been made to correlate the effectiveness factor with the physical properties of the system, its value can be estimated only for few simple cases (30). It is desirable to obtain kinetic data under such conditions, that the value of the effectiveness factors approaches unity. This is generally accomplished by decreasing the particle size. In this experiment the internal diffusion was eliminated by using a small particle size (20-40 mesh).

The effect of Knudsen diffusion was determined by varying the particle size of the catalyst while keeping temperature, residence time and mole ratio constant. Two runs were made at a temperature of 245°C, a residence time of 5.75 gm-cat-hr/gm-mole and a hydrogen/pyridine mole ratio of 40. The effect of particle size of the catalyst on conversion of pyridine have been investigated. Results are shown in Appendix D. In case Knudsen diffusion was affecting the results significantly, changing catalyst diameter should have resulted in significant change in the rate of reaction. Hence, it can be assumed that Knudsen diffusion effects were negligible.

It can be concluded that internal diffusion was negligible at the condition of in this study.

(3) Departure from Plug Flow

The general rate of a catalytic reaction in a flow system based upon unit mass of catalyst is given by the relation,

$$r_A \, dW = F \, dX_A$$

where,

r_A = moles of reactant A converted per (unit time) unit mass of catalyst

F = flow rate of feed, moles per unit time

W = mass of catalyst in the reactor, gms

X_A = mole of A converted per mole of the feed

The reaction rate is usually correlated to composition and temperature at the surface of the catalyst where the catalytic reaction takes place. However, there is a mass and heat transfer film gradient at the catalyst surface (25). Therefore it is desirable to operate at high velocity and small particle size to maintain a small film gradient and thus the temperature and the pressure in the catalyst is the same as the ambient temperature and pressure. If there is a deviation from plug flow the rate equation derived does not apply to the experimental data.

(4) Homogeneous Reactions

The reactants were fed to the reactor to find out as to whether any reaction took place, while the reactor was empty. Using a pyridine partial pressure of 0.03553×10^6 N/m^2, a hydrogen/pyridine mole ratio of 80 and W/F = 0.64 gm-cat-hr/gm-mole, and at 450°C it was found that none of the pyridine was converted. However under the same conditions pyridine was completely converted. It can therefore be concluded that no homogeneous reaction took place.

(5) Variation of Catalyst Activity

It was observed that initially the catalyst had a very high activity when reduced in a stream of hydrogen. However this activity became constant with time and later the catalyst deactivated. A detailed discussion on catalyst deactivation is given in Appendix A. The deactivation of the catalyst may be due to excessive high temperature and to poisoning. The activity of the catalyst used in this study was checked from time to time by repeating some runs. The catalyst was changed if and when it was found that it was deactivated, and constant activity could not be restored by activation.

VI. DISCUSSION

The kinetics of hydrodenitrogenation of pyridine has been carried out over a catalyst containing nickel tungstate on alumina at a hydrogen pressure of 2.928×10^6 N/m^2 and a temperature range of 120-380°C. The investigation obejctive was to study the product distribution as a function of temperature to postulate a general mechanism and to derive a rate expression for hydrogenation of pyridine and to calculate the rate constant.

Many attempts have been made in the past to understand the hydrodenitrogenation process. However, very little work has been published about the mechanism of the process. Most of the work done on hydrodenitrogenation was to understand the process as a whole for a definite set of conditions. The investigations carried out by McIlvried (14) and Sonnemans et al. (15, 16, 17, 18) were the most extensive studies.

- Reaction scheme of hydrogenolysis of pyridine

The products formed from pyridine hydrodenitrogenation were determined as a function of temperature. The reaction time and the molar ratio H_2/py were kept constant. The product distribution is shown in Figure 5-8. The products formed by hydrodenitrogenation of pyridine were piperidine, n-pentylpiperidine, ammonia and pentane. At small hydrogen/pyridine molar ratios pentene, dipentylamine, decane and pentylamine were analyzed. A study of the product

distribution as a function of temperature showed that n-pentylpiperidine was the main intermediate product. This compound was reported by Sonnemans et al.(15, 16). The formation of this product indicated that the most important reaction was not the formation of n-pentylamine by the opening of the piperidine ring, but the disproportionation of two piperidine molecules into ammonia and n-pentylpiperidine. Sonnemans et al.(17) had experimental evidence that the formation of n-pentylpiperidine by alkyl transfer from n-pentylamine to piperidine was found to increase when pentylamine was added. It has been concluded that n-pentylpiperidine and ammonia were formed by ring opening of piperidine followed by a rather fast alkyl transfer from pentylamine to piperidine. In this study, pentylamine was formed in a ratio which did not depend on temperature. The formation of n-pentylpiperidine in considerable amounts suggested the following mechanism

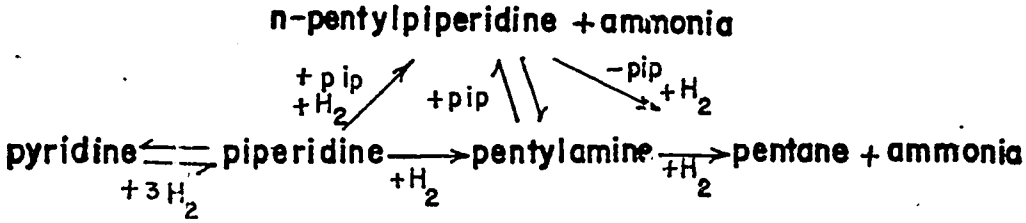

This mechanism has been found to be similar to that obtained by Sonnemans et al.(15).

On the other hand the mechanism disagreed with that postulated by McIlvried (14) who assumed the following reaction scheme:

pyridine → piperidine → n-pentylamine → pentane + ammonia

McIlvried did not analyze for individuals components of the product but only for the nitrogen content in the product.

Aboul-Gheit et al.(6) who studied the hydrodenitrogenation of pyridine in paraffin oil found that the reaction occurred in the following sequence:

pyridine → piperidine → amylamine → pentane + ammonia

At lower temperatures alkyl piperidines were reported to be formed in side reactions and their yield increased with the initial hydrogen pressure.

Another reaction scheme which has been suggested by Satterfield et al.(13) included an equilibrium between pyridine and piperidine. The following scheme was given:

$$\text{pyridine} \underset{-H_2}{\overset{+H_2}{\rightleftharpoons}} \text{piperidine} \xrightarrow{+H_2} \text{pentylpiperidine} \rightarrow \text{pentane} + \text{ammonia} + H_2$$

The mechanism of reaction postulated in this study was the best to fit the experimental data. n-Pentylpiperidine which was the main intermediate product, was reported also by Sonnemans (15). n-Pentylamine which has been found in small amounts compared to n-pentylpiperidine was reported to be the main intermediate by McIlvried (14) and Satterfield et al.(13). Aboul-Gheit et al.(6) who reported that amylamine was the intermediate analyzed alkyl piperidines in the product stream. Therefore, the reaction schemes postulated by McIlvried (14), Aboul-Gheit (6) and Satterfield et al.(13) could not be adopted. On the other hand a part of the reaction

network derived by Sonnemans et al.(15) was found to fit the experimental data of this study.

Hydrogenation of Pyridine

In the present investigation of hydrogenation of pyridine, a first order with respect to pyridine and hydrogen was found by varying the reaction time. The first order was found to indicate increased conversions of pyridine with increase hydrogen/pyridine ratios. Similar observation was reported by Sonnemans et al.(16) and McIlvried (14).

The apparent first order rate constant of pyridine hydrogenation, calculated in this study, was found inversely proportional to the initial partial pressure of pyridine. Similar results were also reported by Sonnemans et al.(16), McIlvried (14), Cox (11) and Shrieber (24).

Cox (6) found a first order kinetics in pyridine to hold, and observed a decrease in the magnitude of the first order rate constant with increased concentration of the nitrogen in the feed.

McIlvried (14), who investigated the hydrogenation of pyridine over a catalyst containing 2.25% nickel, 1.25% cobalt, and 11% molybdenum supported on alumina, reported that the first order in pyridine varied in such a way as to indicate increased inhibition with increased conversions. It was concluded that only ammonia was strongly absorbed on the hydrogenation sites. The apparent first-order reaction rate constant decreased with increased nitrogen concentration in the feed. The fact that the apparent rate constant decreased

with increasing nitrogen concentration indicated that nitrogen compounds were equally strongly adsorbed on the catalyst and suggested that Lingnuir-Hinshelwood kinetics could be used. The general kinetics of the hydrogenation of pyridine investigated in the present study showed a good agreement with those of McIlvried (14) and Sonnemans et al. (16).

The rate equation derived in this study was obtained by the integral method. The experimental data was found to fit the following rate equation:

$$-\frac{d\left[P_{py}\right]}{dt} = \left(k_i + k_s \bar{R}/\left[P_{H_2}^{\circ}\right]\right)\left(\left[P_{py}\right]\left[P_{H_2}\right]\right)$$

The rate expression for hydrogenation of pyridine derived by McIlvried (14) was as follows:

$$-\frac{d\left[P_{py}\right]}{dt} = \frac{4.55\ \pi\ \left[P_{H_2}\right]\left[P_{py}\right]\ \times 10^{-4}}{(1+\bar{R})\ (1+10.5)\left[P_{Am}\right]}$$

The above rate equation was based on the model of equally strong adsorption of reactants and products on the catalyst and Lagmuir type adsorption of pyridine and piperidine.

Sonnemans et al. (16) used the same assumptions to derive a rate equation for pyridine hydrogenation. The following rate equation was found to fit his data

$$-\frac{d\left[P_{py}\right]}{dt} = \frac{k_{ov}}{\left[\overline{P_{py}}^{\circ}\right]}\left[P_{py}\right]\left[P_{H_2}\right]^m$$

where $m = 1.0$ at 250°C

$m = 1.5$ at 300-375°C

The mechanism postulated in this study is the most probable. Further experiments are needed to substantiate a

more definite mechanism.

The order of the hydrogenation of pyridine with respect to pyridine and hydrogen observed in this study seemed to agree with studies done on different types of catalyst. The proposed rate equation was qualitatively similar to those reported by other authors (14, 16).

The activation energy for the hydrogenation of pyridine has not been reported in the literature. However Sonnemans et al. (17) reported activation energies for hydrocracking, alkyl transfer. The activation energy for the hydrogenation of pyridine calculated in this study was 13.691 Kcal/gm mole. Sonnemans et al. (16) reported rate constants for pyridine hydrogenation as a function of temperature. Those values were used to calculate the activation energy. The activation energy obtained from a log k_{ov} vs $1/_T$ plot calculated was 22.445 Kcal/gm-mole.

Comparing the activation energy calculated in this study to that calculated from Sonnemans et al. (16) shows that a somewhat lower value was obtained.

VII. SUMMARY, CONCLUSION AND RECOMMENDATIONS

The kinetics of the hydrodenitrogenation of pyridine over $NiO-WO_3-Al_2O_3$ catalyst was studied under a hydrogen pressure of 2.928×10^6 N/m^2 and over a wide range of temperature in an isothermal fixed bed reactor.

The products were formed in the following order: piperidine, n-pentylpiperidine, ammonia and pentane. Other products such as, dipentylamine, n-pentylamine, pentene and decane were found in traces. Hydrodenitrogenation of pyridine involved an intermediate (n-pentylpiperidine). The intermediate decomposed to pentane and ammonia. A possible reaction mechanism has been postulated.

Hydrogenation of pyridine to piperidine was found to be a first order reaction with respect to both pyridine and hydrogen, but the apparent rate constant was a function of initial partial pressure of pyridine.

The rate equation for the hydrogenation of pyridine over the catalyst was formulated as follows:

$$-\frac{d\left[P_{py}\right]}{dt} = \left(k_i + k_s \bar{R}/\left[P_{H_2}^{\circ}\right]\right)\left[P_{py}\right]\left[P_{H_2}\right]$$

The constants k_i and k_s were calculated at 145, 195, 245 and 280°C.

The activation energies and the frequency factor were calculated at $\bar{R}$ = 40, 50, 60 and 90. The average values were 13.691 Kcal/gm-mole and 5.987×10^{-2} gm-mole/gm-cat-hr-N/m^2 respectively.

In order to understand the mechanism of the hydrodenitrogenation over $NiO-WO_3-Al_2O_3$ better, it is recommended that:

1. Additional kinetic studies must be carried out on: piperidine, n-pentylpiperidine and n-pentylamine.
2. The adsorption behavior of the nitrogen bases and hydrogen on alumina and the nickel containing catalysts should be investigated and the effect of each component of the catalyst on hydrodenitrogenation of pyridine must be studied.
3. Kinetic studies on hydrodesulfurization of thiophene on $NiO-WO_3-Al_2O_3$ has to be carried out in order to understand the activity of the catalyst in hydrodesulfurization reaction.

VIII. NOMENCLATURE

a_m	Catalyst surface area per unit mass m^2/gm
a_p	Average surface area per particle,
C_p	Specific heat of gas, cal/gm-mole-°c
D_{AM}	Average diffusivity of component A
D_p	Catalyst particle diameter, mm.
E_a	Activation energy, K cal/gm-mole.
F	Flow rate of feed, moles/hr.
G	Molal velocity of flow based on the total cross-sectional area of the catalyst bed
H	Molal heat of reaction of component
h_G	Heat transfer coefficient of gas film.
J	Dimensionless Chilton-Colburn factor
k	Thermal conductivity of the gas
k_a	Rate constant for alkyl transfer of piperidine
k_c	Rate constant of consecutive reactions from piperidine
k_d	Rate constant for disproportionation of pentylamine
k_{de}	Rate constant of denitrogenation
K_G	Mass transfer coefficient of gas film
k_h	Rate constant for hydrocracking of piperidine to n-pentylamine
k_i	Reaction rate constant intercept in a plot K_{ov} vs $1/\left[P_{py}^{\circ}\right]$, $\frac{\text{gm-mole}}{\text{gm-cat-hr-N/}_{m^2}}$
k_{ov}	Observed rate constant for hydrogenation of pyridine, $\frac{\text{gm-mole/hr}}{\text{gm-cat-N/}_{m^2}}$

k_s Reaction rate constant slope in a plot of k_{ov} vs $1/\left[\bar{P}_{py}^{\circ}\right]$, $\frac{\text{gm mole}}{\text{gm-cat-hr}}$.

k_o Frequency factor.

k_1 Forward rate constant of hydrogenation of pyridine.

k_{-1} Backward rate constant of hydrogenation of pyridine.

k_2 Rate constant of hydrogenation of piperidine to n-pentylamine.

k_4 Rate constant of alkyl transfer of piperidine to pentylamine.

M_m Average molecular weight of the gas reaction order with respect to hydrogen in pyridine hydrogenation.

n Reaction order with respect to n-pentylamine in disproportionation reaction of pentylamine.

n_1 Overall reaction order of hydrogenation of pyridine

n_c Overall reaction order of consecutive reaction from piperidine

P_i Partial pressure of component i.

Pr Prandtl number.

R Gas constant in cal/gm-mole - °K.

$\bar{R}$ Mole ratio of hydrogen to pyridine.

r Reaction rate, $\frac{\text{gm mole } (N/m^2)}{(\text{gm-cat})(\text{hr})}$.

Re Reynolds number.

r_h Rate of heat transfer of heat of reaction per unit mass of catalyst.

r_{mA} Rate of reaction or mass transfer of A per unit mass of catalyst.

Sc	Schmidt number.
t	Time.
T	Temperature.
T_i	Temperature of the gas - solid interface.
W	Weight of catalyst, gm.
X	Conversion of pyridine or formation of product
Y	Mole fraction.

Greek Symbols

Δ	Finite increment or change of property.
δ	Change in moles per mole of reactant (or product).
μ	Viscosity.
π	Total pressure.
ρ	Density.
ϕ	Shape factor, ratio of actual external surface area available for mass and heat transfer to the total external surface area.

Subscripts

A	Component A in the ambient stream.
A_i	Component in the gas-solid interface
Am	Ammonia.
f	Properties of the average condition of the gas film.
H_2	Hydrogen.
mpa	n-pentylamine.
pip	Piperidine

p.pip n-pentylpiperidine

py pyridine

Superscripts

m Reaction order with respect to hydrogen in hydrogenation of pyridine

o Initial condition

IX. REFERENCES

1. Weiser, O., and S. Landa, "Sulphide Catalysts, their Properties and Applications", Pergamon Press, New York, N.Y., (1973).

2. Kung T. Ng and David M. Hercules, "Studies of Nickel-Tungsten-Alumina Catalysts by X-Ray Photoelectron Spectroscopy", The Journal of Physical Chemistry, Vol. 80, No. 19, (1976).

3. R.J. Williams, R.G. Draper, and B.I. Parsons, "Catalyst for Hydrocracking and Refining Heavy Oils and Tars, Part 1", Mines Branch Technical Bulletin TB-187, Mines and Resources, Ottawa, Canada.

4. Goudriaan, F., Gierman, H., and Vlugter, J.C., "Effect of Hydrogen Sulfied on Hydrogenation of Pyridine", J. Inst. Petrol., London, Vol. 59, No. 565, pp. 40-1, (1973).

5. Frost, C.M., Jensen, H.B., "Hydrodenitrification of Crude Shale Oil", Prepr. Div. Pet. Chem. Am. Chem. Soc., Vol. 18, No. 1, pp. 119-28, (1973).

6. Aboul-Gheit, A.K.; Abdou, I.K., and Mustafa, A., "Hydrodenitrogenation Studies. Part I. Pyridine", Egypt. J. Chem., Vol. 17, No. 5, pp. 617-29, (1974).

7. Agzamova, M., Abdukadyrov, A. Sapozhnikova, E.A., Sultanov, A., and Sultanov, A.S., "Hydrodesulfurization of petroleum products on a modified aluminum-nickel-molybdenum catalyst," Deposited Doc., Viniti 7314-73, (1973).

8. Aboul-Gheit, A.K.; Abdou, I.K., and Mustafa, A., "Hydrodenitrogenation Studies. Part III. Indole", Egypt. J. Chem., Vol. 17, No. 6, pp. 853-67, (1974).

9. Aboul-Gheit, A.K., Abdou, I.K., and Mustafa, A., "Hydrodenitrogenation Studies, Part II. Quinoline," Egypt. J. Chem., Vol. 17, No. 5, pp. 631-44, (1974).

10. Kirk-Othmer, "Encyclopedia of Chemical Technology, 2nd ed." Vol. 11, p. 424, Interscience publisher, N.Y., (1966).

11. Cox, K.E., "The Destructive Catalytic Hydrogenation of certain Heterocyclic Nitrogen Compounds", Ph.D. Thesis, Montana State College, Bozeman, Mont., (1961).

12. C.N. Satterfield and J.F. Cocchetto, "Pyridine Hydrodenitrogenation: An Equilibrium Limitation on the Formation of Piperidine Intermediate", AIChE Journal, Vol. 21, No. 6, pp. 1107-1111, Nov. (1975).

13. C.N. Satterfield, M. Modell, and J.F. Mayer, "Interaction Between Catalytic Hydrosulfurization of Thiophene and Hydrodenitrogenation of Pyridine"; AIChE Journal, Vol. 21, No. 6, pp. 1100-1107, Nov. (1975).

14. H.G. McIlvrid, "Kinetics of the Hydrodenitrification of Pyridine", Ind. Eng. Chem. Process Design Develop., Vol. 10, No. 1, pp. 125-130, (1971).

15. J. Sonnemans, F. Goudriaan and P. Mars, "The Hydrogenolysis of Pyridine on Molydenumoxide Containing Catalysts", The Paper 76, Fifth Intl. Cong. on Catal., Palm Beach, Fla., (1972).

16. J. Sonnemans, G.H. Van Den Berg, and P. Mars, "The Mechanism of Pyridine Hydrogenolysis, on Molybdenum-Containing Catalysts," II. "Hydrogenation of Pyridine to Piperidine", J. Cat., Vol. 31, p. 220, (1973).

17. Sonnemans, J., W.J. Neyens and P. Mars, "IV. The Conversion of Piperidine", Ibid., Vol. 34, p. 230, (1974).

18. Sonnemans, J. and P. Mars, "III. Cracking Hydrocracking, Dehydrogenation and Disproportionation of pentylamine", Ibid., Vol. 34, p. 215, (1974).

19. Flinn, R.A., D.A. Larson, and H.B. Beuther, "How Easy is Hydrodenitrogenation", Hydrocarbon Process. Petrol. Refiner, Vol. 42, No. 9, pp. 129-132, (1963).

20. Doelman, J. and J.C. Vlugter, "Model Studies on Catalytic Hydrogenation of Nitrogen containing Oils", World Petrol. Congr., Proc. 6th, Frankfurt, Sect. III, pp. 247-257, (1963).

21. Beuther, H. and O.A. Larson, "Role of Catalytic Metals in Hydrocracking", Ind. and Eng'g Chem., Proc. Desn and Dev., Vol. 4, No. 2, p. 177-181, (1965).

22. Beugeling, T, M. Boduszyuski, F. Goudriaan, and J.W.M. Sonnemans, "Gas-liquid Chromatographic Analysis of Products Formed by the Hydrogenolysis of Pyridine", Analytical Letters, Vol. 4, No. 11, pp. 727-735, (1971).

23. Laidler, K.J., "Chemical Kinetics", 2nd ed., p. 2, McGraw-Hill Book Co., N.Y., (1965).

24. Shreiber, G.P., Ph.D. Thesis, Montana State College, Bozeman, Mont., (1961).

25. J.B. McCullough et al., J. Am. Chem. Soc., Vol. 79, p. 4289 (1957).

26. Yang, K.H., O.A. Hougen, "Determination of Mechanism of Catalyzed Gaseous Reactions", Chem. Eng'g Progress, Vol. 46, No. 3, pp. 146-157, (1950).

27. Smith, J.M., "Chemical Engineering Kinetics", 1st ed., McGraw-Hill, New York, pp. 231-250 (1970).

28. Yoshida, F., Ramaswami, D., and Hougen, O.A., "Temperature and Partial at the Surface of Catalyst Particles", A.I.Ch.E., Vol. 8, No. 1, pp. 5-11, (1962).

29. Goudriaan, F., "Hydrodenitrogenation of pyridine", doctoral thesis, Twente Technical Institute, The Netherlands, (1974).

30. Hougen, O.A., and Watson, K.M. "Chemical Process Principles", Part III, John Wiley and Sons, New York, p. 996, (1947).

X. APPENDIX

(A) Properties of the catalyst

Nickel-tungsten-alumina catalysts are important, because of their catalytic action in hydrodesulfurization, hydrocracking, and hydrogenation processes. (1)

Kung and Hercules (2) have studied several catalysts supplied by Harsaw Chemical Co. various treatments such as reduction and sulfiding were carried out on the catalysts as a function of time and temperature. X-ray photoelectron spectroscopy have been used (ESCA) to detect the kind of species available on the surface of the catalyst. When the catalyst was reduced at 500°C in hydrogen, tungsten remained in the +6 oxidation state and was not reduced even after prolonged treatment. On the other hand, nickel was readily reduced to nickel metal.

The nickel/tungsten/alumina catalyst (Ni 4303) was reduced in H_2 at 450°C. The percentage reduction for both nickel and tungsten is plotted as a function of time in Figure 4.

Reduction experiments of the catalyst indicated that nickel was present on the surface as $NiAl_2O_4$ and Ni_2O_3 while tungsten was present as W(+6) species. A surface interaction complex which, probably formed during calcination, was proposed as follows:

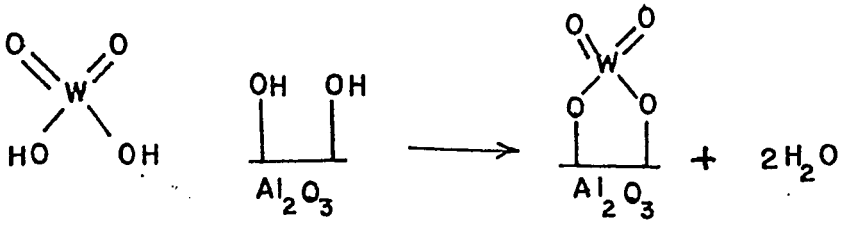

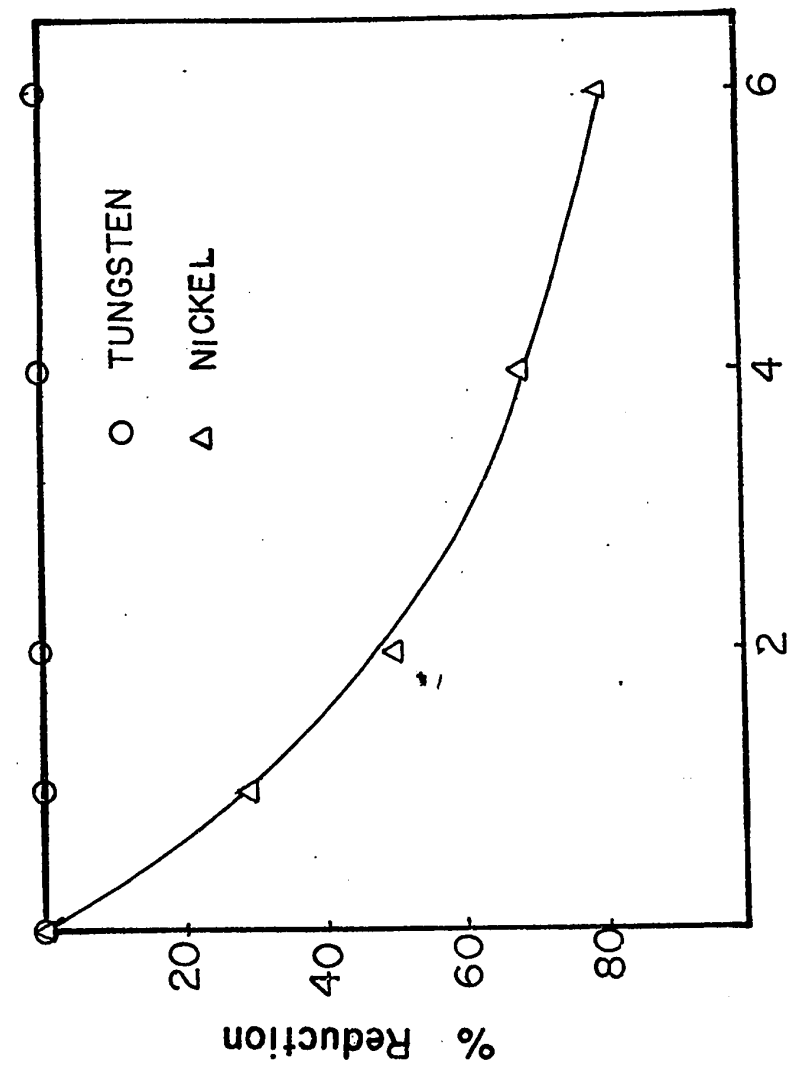

Fig. 4: Reductin of nickel tungsten catalyst at 450 °C

The catalyst used in the present study (Ni 4303) was obtained from Harsaw Chemical Co. This catalyst had been prepared by impregnating nickel and tungsten onto a γ-Al_2O_3 surfaces in the form of oxides. The composition of the catalyst by weight was 6% of Ni and 19% of W.

Before using this catalyst, it was reduced for 48 hrs at 450°C with a hydrogen flow rate 60 cm^3/min.

(B) External Diffusion (Drop in Partial Pressure)

The data for this estimation of the external diffusion are obtained from Run No. 142. The conditions which apply to this evaluation are:

Temp. = 280°C

W/F = 3.77 gm cat-hr/gm-mole

$\bar{R}$ = 50

ϕ = shape factor or sphericity

= 0.9 for irregular granules

G_m = molal mass velocity of feed based on the total cross section of the catalyst bed in moles/hr-cm^2

$$= \frac{2.4084 \text{ moles}}{\pi/4\ (1/2 \times 2.54)^2} = 1.9012 \text{ moles/hr-cm}^2$$

W = 9.08849 gms

a_m = surface area of the catalyst particle per unit mass of the catalyst

= 3.5 m^2/gm

= 35000 cm^2/gm

(F_j) in = flow rate of component j in the feed

(F_j) out = flow rate of component j in the product

(Y_j) in = mole fraction of component j in the feed

(Y_j) out = mole fraction of component j in the product

Y_j = mole fraction of component j at the interface $\simeq$

$$\frac{(Y_j) \text{ in} + (Y_j) \text{ out}}{2}$$

r_{mj} = molal reaction rate of component j per unit mass of the catalyst

R_j = dimentionless terms of component j

$$= \frac{r_{mj}}{a_m \phi G_m}$$

$$= \frac{r_{mj}}{(35000)(0.9)(1.9012)}$$

for example

r_{mj} = molal reaction rate of products per unit mass of the catalyst

$$= \frac{0.88 \times 2.4084 \text{ moles/hr}}{9.08849 \text{ gm}} = 0.223 \text{ moles/gm-hr}$$

$$R_{Py} = \frac{0.233}{(35000)(0.9)x(1.9012)} = 3.89 \times 10^{-6}$$

$$Y_j = \frac{1 + 0.12}{2} = 0.56$$

$$\frac{R_{Py}}{Y_j} = \frac{3.89 \times 10^{-6}}{0.56} = 6.947 \times 10^{-6}$$

The value of $\Delta P_{py}/P_{py}$ is obtained from $\Delta P_j/P_j$ versus R_j/Y_j plot given in Figure 2 by Yoshida et al (28). Since the value is less than 0.001, the external diffusion effects are neglected.

(C) Temperature Drop from Catalyst Particle to Ambient Gas Stream

From Appendix (B)

$$r_{mf} = \frac{0.88 \times 2.4084}{9.08849} = 0.223 \text{ moles /gm-hr.}$$

$\phi = 0.9$

$G_m = 1.9012$ moles/hr-cm^2

$a_m = 35000$ cm^2/gm

ΔH_f of products

$= \Delta H_f C_5 + \Delta H_f NH_3 - (\Delta H_f py)$

$= -[(41.36) + (11.04)] - 23.95$

$\Delta H_f = -76.35$ K cal/mole

$$C_p = \sum_{i=1}^{5} (C_p)i \; Y_i$$

$= (0.22 \times 19.06 + 0.292 \times 28.73 + 0.487 \times 8.24)$

$= 16.59$ cal/gm-mole °C

$$Q_f = \frac{r_{mf} (\Delta H)}{a_m \phi C_p G_m}$$

$$Q_f = \frac{0.223 \times 76350}{16.59 \times 35000 \times 0.9 \times 1.9012}$$

$= 0.0171$

Since from Figures 3 and 4 of Yoshida et al (28) at Q_f = 0.0171 ΔT is less than 0.1°C, the catalyst surface temperature effect can be neglected.

(D) Internal Diffusion

Effect of catalyst particle diameter and of changing feed velocity is shown in Table D-1.

Table D-1

Temp. = 245°C, $\bar{R}$ = 40, W/F = 5.75 gm-cat-hr/gm-mole

Particle Size	$F_{py_o} \times 10^{-4}$ mole/min	Weight of catalyst gm	Conversion X
20/40 mesh	6.419	9.08849	0.71
20/40 mesh	3.893	5.51130	0.708
60/80 mesh	6.419	9.08849	0.715

(E) Sample Calculations and Material Balance

The following is a sample calculation of each of the kinetic parameters of hydrodenitrogenation of pyridine.

The data shown in Table (1-4) is the normalized mole fractions calculated from the area under the peak. The calibration curves of moles of component against area under the peak are straight lines. The slopes of these calibration lines were used to calculate the number of moles from the area under the peak. A computer program was used to do the calculation of the normalized mole fractions.

Experimental data below is taken from Run No. 15

Total pressure = 2.928 x 10^6 N/m^2

F_{pyo} = 30.95 c.c/min = 0.0828 moles/hr

$F_{H_2^\circ}$ = 900 c.c/min = 2.4 moles/hr

P_{pyo} = P total x X_{py} = 0.09760 x 10^6 N/m^2

$P_{H_2^\circ}$ = P total x X_{H_2} = 2.830 x 10^6 N/m^2

Weight of Catalyst = 9.08849 gm

Temperature = 260°C

Mole ratio $\bar{R} = \frac{[Hy^\circ]}{[py^\circ]} = \frac{2.4}{0.0828} = 29.$

$W/F = \frac{9.08849}{(2.41 + 0.0828)} = 3.6 \frac{\text{gm-cat-hr}}{\text{gm-mole}}$

Component	Area	Slope	No. of moles	ϕ_N moles
pyridine	11.16	0.004	0.04464	0.54
piperidine	3.81	0.003904	0.01487	0.18
n-pentyl piperidine	4.96	0.004	0.01984	0.24
ammonia	0.33	0.00988	0.00326	0.04

Carbon balance based on 1 hour.

Atoms of carbon in = 5 (0.08289) = 0.41445 atoms.

Atoms of carbon out = 5 [0.04464 + 0.01487 + 2 (0.01984)]

= 0.4959

% error = $\frac{0.41445 - 0.4959}{0.41445}$ x 100 = 19%

Nitrogen balance based on 1 hr.

Atoms of nitrogen in = 0.08289 = 0.08289 atoms

Atoms of nitrogen out = 0.04464 + 0.01487 + 0.01984 + 0.00326

= 0.08261 atoms

% error = $\frac{0.08289 - 0.08261}{0.08289}$ x 100 = 0.33%

Figure 24 A typical analysis of products.

1- Ammonia

2- Piperidine

3- Pyridine

4- N- Pentyl piperidine

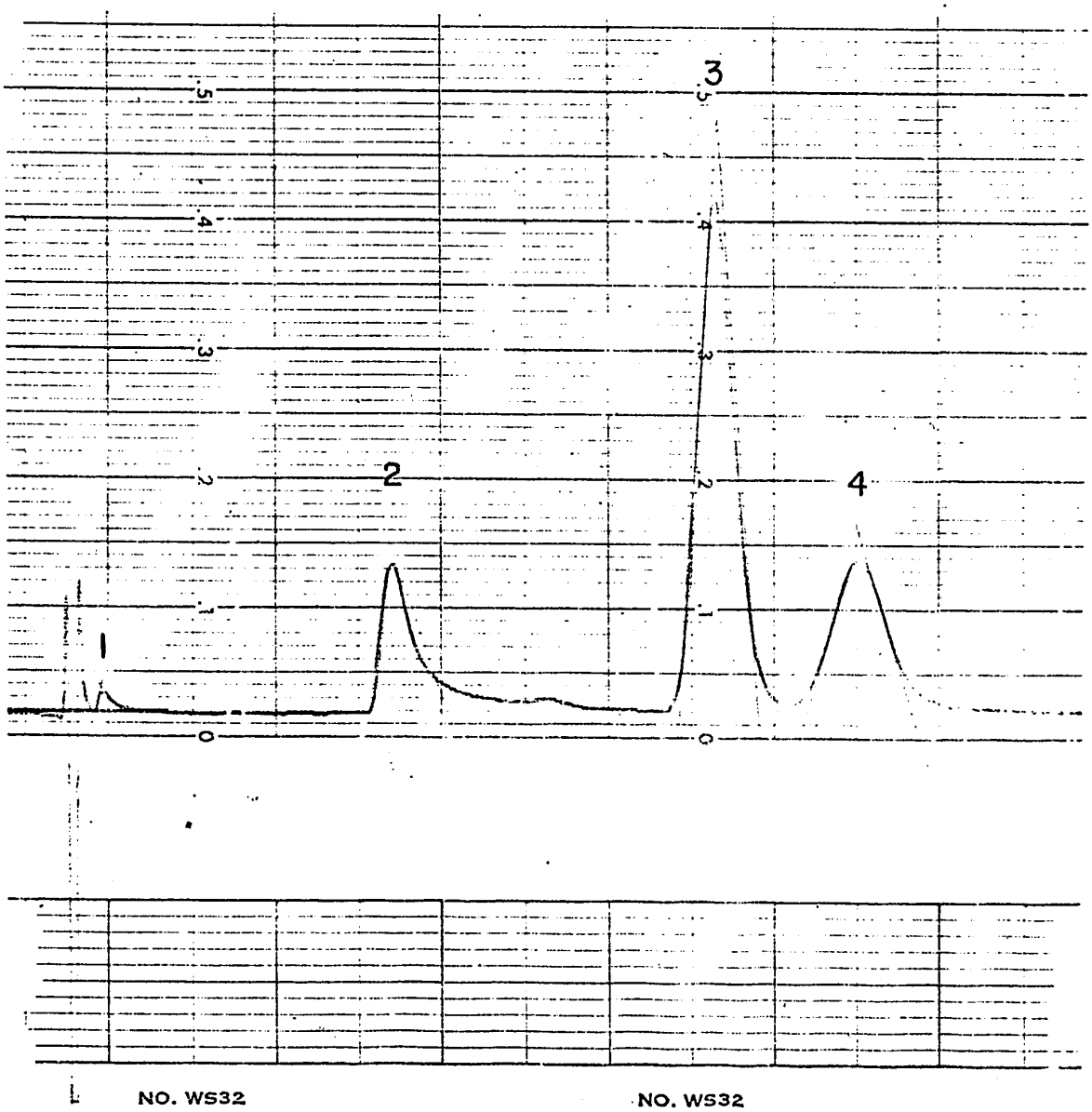

F-1 Experimental Data

The effects of temperature on product distribution at W/F = 3.6 gm cat - hr/gm-mole, in the temperature range of 120-380°C, at hydrogen/pyridine molar ratios of 29, 40, 60 and 80.

TABLE 1-I Results of Effect of Temperature on Product Distribution

F_{pyo} = 0.08289 moles/hr Initial partial pressure of hydrogen = 0.0976 x $10^6 N/m^2$

$F_{H_2 o}$ = 2.4038 moles/hr Initial partial pressure of pyridine = 2.8304 x $10^6 N/m^2$

mole ratio = 29 W/F = 3.6 gm-cat-hr/gm-mole

Run No.	Temp. °C	moles PYR	moles pip	moles p.pip	moles ammonia	moles pentane
1	122	0.0808	0.00207	-	-	-
2	133	0.07999	0.00289	-	-	-
3	140	0.08019	0.00269	-	-	-
4	150	0.08023	0.00265	-	-	-
5	160	0.07875	0.00414	-	-	-
6	172	0.07792	0.00496	-	-	-
7	180	0.07543	0.00745	-	-	-
8	191	0.07253	0.01036	-	-	-
9	200	0.06904	0.01096	0.00121	-	-
10	215	0.06376	0.01624	0.00121	-	-
11	220	0.06214	0.01746	0.00162	-	-
12	228	0.06174	0.01786	0.00162	-	-
13	240	0.05524	0.01949	0.00650	-	-
14	252	0.05212	0.01671	0.00954	0.00119	-
15	260	0.04073	0.01357	0.01810	0.00301	-
16	270	0.02349	0.01119	0.03431	0.00405	-
17	280	0.01422	0.00765	0.04230	0.00528	-
18	289	0.00984	0.00765	0.04303	0.00948	0.00211
19	300	0.00932	0.00559	0.03879	0.01342	0.00745
20	315	0.00753	0.005322	0.03547	0.026166	0.01419
21	330	0.00549	0.00439	0.01977	0.04887	0.03130
22	340	0.00590	0.00412	0.01357	0.0567	0.0378
23	355	0.00329	-	0.00856	0.06655	0.05338
24	360	0.00407	0.00135	0.002718	0.07069	0.057096

TABLE 1-II Results of Effect of Temperature on Product Distribution

Initial partial pressure of pyridine = 0.0976×10^6 N/m^2

Initial partial pressure of hydrogen = 2.8304×10^6 N/m^2

Mole ratio = 29

W/F = 3.6 gm-cat-hr/gm-moles

Run No.	Temp. °C	$\phi PYR/\phi PYR_o$	$\phi pip/\phi PYR_o$	$\phi N\text{-}P.\ pip/\phi PYR_o$	$\phi Ammonia/\phi PYR_o$	$\phi Pentane/\phi PYR_o$
1	122	0.975	0.025	-	-	-
2	133	0.965	0.035	-	-	-
3	140	0.9675	0.0325	-	-	-
4	150	0.968	0.032	-	-	-
5	160	0.95	0.05	-	-	-
6	172	0.94	0.06	-	-	-
7	180	0.91	0.09	-	-	-
8	191	0.875	0.125	-	-	-
9	200	0.850	0.135	0.015	-	-
10	215	0.785	0.200	0.015	-	-
11	220	0.765	0.215	0.02	-	-
12	228	0.760	0.220	0.02	-	-
13	240	0.68	0.240	0.08	-	-
14	252	0.655	0.21	0.12	0.015	-
15	260	0.54	0.18	0.24	0.04	-
16	270	0.315	0.15	0.46	0.075	-
17	280	0.195	0.105	0.58	0.10	0.02
18	289	0.135	0.105	0.59	0.130	0.04
19	300	0.125	0.075	0.52	0.18	0.10
20	315	0.085	0.06	0.40	0.295	0.16
21	330	0.05	0.04	0.18	0.445	0.285
22	340	0.05	0.035	0.115	0.48	0.32
23	355	0.025	-	0.065	0.505	0.405
24	360	0.03	0.01	0.02	0.52	0.42

TABLE 2-I Results of Effect of Temperature on Product Distribution

Mole ratio = 40 F_{pyo} = 0.0606 mole/hr Initial Partial pressure of py = 0.0714×10^6 N/m^2

F_{H_2O} = 2.424 moles/hr Initial Partial pressure of H_2 = 2.8566×10^6 N/m^2

W/F = 3.6 $\frac{\text{gm-cat-hr}}{\text{gm-mole}}$

Run No.	Temp. °C	moles pyr	moles pip	moles p. pip	moles ammonia	moles pentane
25	140	0.05823	0.00242	-	-	-
26	153	0.05731	0.00333	-	-	-
27	160	0.05580	0.00484	-	-	-
28	169	0.05307	0.00757	-	-	-
29	180	0.05216	0.00849	-	-	-
30	191	0.04943	0.01122	-	-	-
31	200	0.04339	0.01248	0.00356	-	-
32	215	0.03814	0.015966	0.00502	-	-
33	220	0.03394	0.01638	0.00760	0.00058	-
34	227	0.02881	0.01613	0.01065	0.00201	-
35	240	0.02425	0.0141	0.01466	0.00282	0.000564
36	250	0.01360	0.01147	0.02322	0.00373	0.00133
37	260	0.00991	0.01043	0.02581	0.00469	0.00130
38	275	0.00438	0.00850	0.03196	0.00489	0.00206
39	280	0.00334	0.00541	0.03248	0.00721	0.003366
40	292	0.00203	0.00611	0.0321	0.00509	0.00458
41	300	0.00273	0.00518	0.02702	0.01200	0.007914
42	310	0.00165	0.00331	0.02484	0.01490	0.01048
43	320	0.00109	0.00400	0.02074	0.02911	0.01783
44	330	0.00166	0.00373	0.015372	0.03656	0.02575
45	340	0.00090	0.00181	0.00818	0.04822	0.03184
46	360	0.00048	0.00097	0.00291	0.05337	0.03930

TABLE 2-II Results of Effect of Temperature on Product Distribution

Initial partial pressure of pyridine = 0.0714×10^6 N/m^2

Initial partial pressure of hydrogen = 2.8556×10^6 N/m^2

Mole ratio = 40

W/F = 3.6 gm-cat-hr/gm-mole

Run No.	Temp. °C	$\phi PYR/\phi PYR_o$	$\phi pip/\phi PYR_o$	ϕN-P. pip/ϕPYR_o	ϕAmmonia/ϕPYR_o	ϕPentane/ϕPYR_o
25	140	0.96	0.04	-	-	-
26	153	0.945	0.055	-	-	-
27	160	0.92	0.08	-	-	-
28	169	0.875	0.125	-	-	-
29	180	0.86	0.14	-	-	-
30	191	0.815	0.185	-	-	-
31	200	0.73	0.21	0.06	-	-
32	215	0.645	0.27	0.085	-	-
33	220	0.58	0.28	0.130	0.010	-
34	227	0.5	0.28	0.185	0.035	-
35	240	0.43	0.25	0.26	0.05	0.01
36	250	0.255	0.215	0.435	0.070	0.025
37	260	0.19	0.2	0.495	0.09	0.025
38	275	0.085	0.165	0.62	0.095	0.04
39	280	0.065	0.105	0.63	0.14	0.055
40	292	0.04	0.12	0.63	0.17	0.09
41	300	0.045	0.095	0.495	0.22	0.145
42	310	0.03	0.06	0.45	0.27	0.19
43	320	0.015	0.055	0.285	0.4	0.245
44	330	0.02	0.045	0.185	0.44	0.31
45	340	0.01	0.02	0.09	0.53	0.35
46	360	0.005	0.01	0.03	0.55	0.405

TABLE 3-I Results of Effect of Temperature on Product Distribution

F_{pyo} = 0.040875 mole/hr Initial partial pressure of pyridine 0.04800 x 10^6 N/m^2

F_{H_2O} = 2.45 moles/hr Initial partial pressure of hydrogen 2.88 x 10^6 N/m^2

Mole Ratio = 60 W/F = 3.6 gm-cat-hr/gm-mole

Run No.	Temp. °C	moles PYR	moles pip	moles p.pip	moles ammonia	moles pentane
47	140	0.03760	0.00327	-	-	-
48	148	0.03637	0.00449	-	-	-
49	160	0.03535	0.00551	-	-	-
50	165	0.03433	0.00654	-	-	-
51	180	0.03167	0.00817	0.00102	-	-
52	190	0.02603	0.01181	0.00220	-	-
53	200	0.02303	0.01342	0.00360	-	-
54	212	0.01766	0.01456	0.00660	-	-
55	220	0.00680	0.01526	0.01471	-	-
56	235	0.00480	0.01422	0.01653	-	-
57	240	0.00347	0.01285	0.01719	0.00121	-
58	250	0.00240	0.01115	0.01819	0.00257	-
59	260	0.00260	0.01059	0.01737	0.00364	0.00052
60	270	0.00174	0.01048	0.01650	0.00621	0.00388
61	280	0.00226	0.00907	0.01588	0.01134	0.00680
62	293	0.00182	0.00652	0.01303	0.01825	0.01251
63	300	0.00159	0.00637	0.01115	0.01966	0.01434
64	307	0.00061	0.00429	0.01073	0.02820	0.01747
65	320	0.00061	0.00337	0.00705	0.02789	0.02023
66	330	-	0.00156	0.00625	0.03158	0.02313
67	340	-	0.00139	0.00312	0.03821	0.02675

TABLE 3-II Results of Effect of Temperature on Product Distribution

Initial partial pressure of pyridine = 0.048×10^6 N/m^2

Initial partial pressure of hydrogen = 2.88×10^6 N/m^2

Mole ratio = 60

W/F = 3.6 gm-cat-hr/gm-mole

Run No.	Temp. °C	$\phi PYR/\phi PYR_o$	$\phi pip/\phi PYR_o$	$\phi N\text{-}P.\ pip/\phi PYR_o$	$\phi Ammonia/\phi PYR_o$	$\phi Pentane/\phi PYR_o$
47	140	0.92	0.08	-	-	-
48	148	0.89	0.11	-	-	-
49	160	0.865	0.135	-	-	-
50	165	0.84	0.16	-	-	-
51	180	0.775	0.2	0.025	-	-
52	190	0.65	0.295	0.055	-	-
53	200	0.575	0.335	0.09	-	-
54	212	0.455	0.375	0.17	-	-
55	220	0.185	0.415	0.40	-	-
56	235	0.135	0.40	0.465	-	-
57	240	0.1	0.37	0.495	0.035	-
58	250	0.07	0.325	0.53	0.075	-
59	260	0.075	0.305	0.5	0.105	0.015
60	270	0.045	0.27	0.425	0.160	0.10
61	280	0.05	0.2	0.35	0.25	0.15
62	293	0.035	0.125	0.25	0.35	0.24
63	300	0.03	0.12	0.21	0.37	0.27
64	307	0.01	0.07	0.175	0.46	0.285
65	320	0.01	0.055	0.115	0.455	0.33
66	330	-	0.025	0.1	0.505	0.37
67	340	-	0.02	0.045	0.55	0.385

TABLE 4-I Results of Effect of Temperature on Product Distribution

F_{pyo} = 0.03026 moles/hr Initial partial pressure of pyridine = 0.0361 x 10^6 N/m^2

F_{H_2O} = 2.421 moles/hr Initial partial pressure of hydrogen = 2.892 x 10^6 N/m^2

Mole Ratio = 80 W/F = 3.6 gm-cat-hr/gm-mole

Run No.	Temp. °C	moles PYR	moles pip	moles p.pip	moles ammonia	moles pentane
68	120	0.02875	0.00151	-	-	-
69	132	0.02754	0.00272	-	-	-
70	140	0.02648	0.00378	-	-	-
71	150	0.02496	0.00529	-	-	-
72	160	0.02451	0.00575	-	-	-
73	173	0.02300	0.00725	-	-	-
74	180	0.02007	0.00913	0.00074	-	-
75	192	0.01218	0.01379	0.00337	-	-
76	200	0.01052	0.01365	0.00426	-	-
77	210	0.00545	0.01293	0.00885	-	-
78	220	0.00323	0.00686	0.01683	-	-
79	230	0.00199	0.00519	0.01890	0.00053	-
80	240	0.00205	0.00360	0.01929	0.0009	-
81	248	0.00130	0.00286	0.01887	0.00221	0.00078
82	260	0.00108	0.00272	0.01756	0.00422	0.00163
83	270	0.00066	0.00216	0.01731	0.00932	0.00382
84	280	0.00075	0.00227	0.01343	0.01324	0.00813
85	293	-	0.00118	0.01022	0.01672	0.01121
86	300	-	0.00264	0.00746	0.01996	0.01470
87	312	-	0.0005	0.00249	0.02646	0.02047
88	320	-	-	0.00154	0.02804	0.02186

TABLE 4.II Results of the Effect of Temperature on Product Distribution

Initial partial pressure of pyridine = 0.0361 x 10^6 N/m^2

Initial partial pressure of hydrogen = 2.892 x 10^6 N/m^2

Mole Ratio = 80

W/F = 3.6 gm-cat-hr/gm-mole

Run No.	Temp. °C	$\phi PYR/\phi PYR_o$	$\phi pip/\phi PYR_o$	$\phi N\text{-}P.\ pip/\phi PYR_o$	$\phi Ammonia/\phi PYR_o$	$\phi Pentane/\phi PYR_o$
68	120	0.95	0.05	-	-	-
69	132	0.91	0.09	-	-	-
70	140	0.875	0.125	-	-	-
71	150	0.825	0.175	-	-	-
72	160	0.81	0.19	-	-	-
73	173	0.76	0.24	-	-	-
74	180	0.670	0.305	0.025	-	-
75	192	0.415	0.47	0.115	-	-
76	200	0.37	0.48	0.15	-	-
77	210	0.2	0.475	0.325	-	-
78	220	0.12	0.255	0.625	-	-
79	230	0.075	0.195	0.71	0.02	-
80	240	0.08	0.14	0.75	0.035	-
81	248	0.05	0.11	0.725	0.085	0.03
82	260	0.04	0.10	0.645	0.155	0.06
83	270	0.02	0.065	0.52	0.28	0.115
84	280	0.02	0.060	0.355	0.35	0.215
85	293	-	0.03	0.26	0.425	0.285
86	300	-	0.04	0.17	0.455	0.335
87	312	-	0.01	0.05	0.530	0.41
88	320	-	-	0.03	0.545	0.425

F-2 The effect of hydrogen/pyridine molar ratio on conversion of pyridine and formation of piperidine, n-pentyl piperidine, pentane and ammonia at W/F = 3.6 gm-cat-hr/gm-mole.

TABLE 5. The Effect of Mole Ratio on Conversion of Pyridine.

W/F = 3.6 gm-cat-hr/gm-mole

Temperature °C	Mole Ratio $\bar{R}$	Conversion X
140	29	0.03
140	40	0.04
140	60	0.075
140	80	0.125
160	29	0.05
160	40	0.08
160	60	0.135
160	80	0.19
180	29	0.09
180	40	0.14
180	60	0.225
180	80	0.325
220	29	0.15
220	40	0.27
220	60	0.44
220	80	0.63

TABLE 6. The Effect of Mole Ratio on Conversion to Piperidine

W/F = 3.6 gm-cat-hr/gm-mole

Temperature °C	Mole Ratio $\overline{R}$	Conversion X
140	29	0.025
140	40	0.04
140	60	0.08
140	80	0.125
160	29	0.05
160	40	0.08
160	60	0.135
160	80	0.185
180	29	0.09
180	40	0.14
180	60	0.2
180	80	0.295

TABLE 7. The Effect of Mole Ratio on Conversion to N-pentylpiperidine

W/F = 3.6 gm-cat-hr/gm-mole

Temperature °C	Mole Ratio $\overline{R}$	Conversion X
200	29	0.015
200	40	0.06
200	60	0.09
200	80	0.15
220	29	0.02
220	40	0.14
220	60	0.4
220	80	0.625
240	29	0.08
240	40	0.26
240	60	0.495
240	80	0.75

TABLE 8. The Effect of Mole Ratio on Conversion to Ammonia

W/F = 3.6 gm-cat-hr/gm-mole

Temperature °C	Mole Ratio $\overline{R}$	Conversion X
260	29	0.04
260	40	0.09
260	60	0.105
260	80	0.155
280	29	0.1
280	40	0.14
280	60	0.25
280	80	0.35
300	29	0.18
300	40	0.22
300	60	0.37
300	80	0.455
320	29	0.33
320	40	0.4
320	60	0.48
320	80	0.545

TABLE 9. The Effect of Mole Ratio on Conversion to Pentane

W/F = 3.6 gm-cat-hr/gm-mole

Temperature °C	Mole Ratio $\overline{R}$	Conversion X
280	29	0.02
280	40	0.06
280	60	0.145
280	80	0.215
300	29	0.1
300	40	0.145
300	60	0.27
300	80	0.33
320	29	0.2
320	40	0.24
320	60	0.33
320	80	0.425

F-3 The effect of residence time on conversion of pyridine at temperatures 145, 195, 245 and 280°C and hydrogen/pyridine molar ratios = 40, 50, 60, 90.

TABLE 10. The Effect of Residence Time on Conversion of Pyridine at 145°C

Run No.	Temp. °C	F_{pyo} x10^{-4} mole/min	F_{H_2O}x10^{-2} mole/min	F_ox10^{-2} mole/min	Mole Ratio $\bar{R}$	W gm	W/F gm-cat-hr/ gm-mole	Conv. X
89	145	4.910	1.964	2.013	40	9.08849	7.52	0.057
90		6.473	2.567	2.631			5.75	0.042
91		7.812	3.125	3.203			4.73	0.032
92		3.973	1.589	1.629			9.29	0.067
93	145	4.80	2.401	2.449	50	9.08849	6.18	0.055
94		6.25	3.125	3.1875			4.75	0.046
95		7.857	3.935	4.013			3.77	0.036
96		3.973	1.986	2.026			7.48	0.066
97	145	4.727	2.834	2.882	60	9.08849	5.25	0.057
98		6.473	3.877	3.942			3.84	0.042
99		7.812	4.705	4.783			3.16	0.035
100		4.017	2.410	2.450			6.18	0.069
101	145	4.799	4.321	4.369	90	9.08849	3.46	0.054
102		6.249	5.625	5.687			2.66	0.043
103		7.812	7.026	7.105			2.13	0.03
104		3.973	3.575	3.615			4.19	0.062

TABLE 11. The Effect of Residence Time on Conversion of Pyridine at 195°

Run No.	Temp. °C	F_{pyo} x10^{-4} mole/min	F_{H_2O}x10^{-2} mole/min	F_ox10^{-2} mole/min	Mole Ratio $\bar{R}$	W gm	W/F gm-cat-hr/ gm-mole	Conv. X
105	195	6.419	3.848	3.915	40	9.08849	3.87	0.170
106		6.696	2.678	2.745			5.51	0.255
107		5.2	2.080	2.145			7.06	0.325
108		7.589	3.035	3.111			4.86	0.22
109	195	3.995	1.997	2.037	50	9.08849	7.46	0.395
110		6.428	3.214	3.278			4.62	0.25
111		4.714	2.357	2.404			6.30	0.32
112		7.812	3.906	3.984			4.05	0.21
113	195	3.973	2.384	2.423	60	9.08849	6.25	0.37
114		6.419	3.851	3.916			3.86	0.22
115		4.687	2.812	2.859			5.29	0.31
116		7.812	4.687	4.765			3.17	0.185
117	195	4.107	3.696	3.737	90	9.08849	4.05	0.30
118		6.473	5.825	5.890			2.57	0.21
119		4.759	4.283	4.338			3.49	0.26
120		7.857	7.071	7.228			2.09	0.160

TABLE 12. The Effect of Residence Time on Conversion of Pyridine at 245°C

Run No.	Temp. °C	F_{pyo} x10^{-4} mole/min	F_{H_2O} x10^{-2} mole/min	F_o x10^{-2} mole/min	Mole Ratio $\bar{R}$	W gm	W/F gm-cat-hr/ gm-mole	Conv. X
121	245	3.893	1.557	1.596	40	9.08849	9.49	0.885
122		4.7093	1.884	1.931			7.84	0.84
123		6.419	2.568	2.632			5.75	0.71
124		8.080	3.232	3.313			4.57	0.63
125	245	3.875	1.019	1.976	50	9.08849	7.66	0.85
126		5.058	2.529	2.579			5.87	0.76
127		6.584	3.292	3.358			4.51	0.7
128		7.910	3.955	4.034			3.75	0.6
129	245	4.763	2.858	2.905	60	9.08849	5.21	0.79
130		4.151	2.491	2.532			5.98	0.84
131		6.562	3.937	4.003			3.78	0.65
132		8.035	4.821	4.901			3.09	0.58
133	245	3.928	3.535	3.575	90	9.08849	4.23	0.76
134		4.749	4.275	4.322			3.50	0.685
135		7.901	7.111	7.150			2.10	0.55
136		6.482	5.834	5.898			2.56	0.58

TABLE 13. The Effect of Residence Time on Conversion of Pyridine at 280°C

Run No.	Temp. °C	F_{pyo} x10^{-4} mole/min	F_{H_2O} x10^{-2} mole/min	F_o x10^{-2} mole/min	Mole Ratio $\bar{R}$	W gm	W/F gm-cat-hr/ gm-mole	Conv. X
137	280	6.696	2.678	2.745	40	9.08849	5.51	0.91
138		7.870	3.148	3.226			4.69	0.88
139		3.892	1.557	1.596			9.49	0.98
140		5.178	2.071	2.123			7.13	9.65
141	280	6.214	3.107	3.169	50	9.08849	4.78	0.94
142		7.870	3.935	4.014			3.77	0.88
143		3.906	1.953	1.992			7.60	0.98
144		4.763	2.381	2.429			6.23	0.97
145	280	6.415	3.849	3.913	60	9.08849	3.87	0.93
146		3.790	2.274	2.312			6.55	0.98
147		4.763	2.858	2.905			5.21	0.98
148		7.870	4.722	4.801			3.15	0.90
149	280	6.317	5.685	5.748	90	9.08849	2.63	0.9
150		8.080	7.272	7.353			2.06	0.86
151		3.727	3.355	3.392			4.4	0.98
152		4.763	4.287	4.334			3.49	0.95

F-4 Calculation of integrated rate expression as a function of residence time at temperatures of 145, 195, 245 and 280°C and hydrogen/pyridine molar ratios of 40, 50, 60 and 90.

TABLE 14. Calculation of Integrated Rate Expression as a Function of Residence Time at 145°C

Temp °C	Mole Ratio $\bar{R}$	Conversion X	$\ln\frac{(\bar{R} - 3X)}{\bar{R}(1-X)}$	W/F gm-cat-hr/ gm-mole
145	40	0.01	0.0093	1.35
		0.02	0.0186	2.7
		0.03	0.0297	4.05
		0.04	0.0430	5.5
		0.05	0.0475	8.1
145	50	0.01	0.0095	1.05
		0.02	0.019	2.15
		0.03	0.0287	3.20
		0.04	0.0384	4.15
		0.05	0.0483	5.4
		0.07	0.0684	7.1
145	60	0.02	0.0192	1.85
		0.03	0.029	2.75
		0.04	0.0388	3.65
		0.05	0.00488	4.5
		0.08	0.0794	7.4
145	90	0.02	0.0195	1.30
		0.04	0.0395	2.65
		0.06	0.0599	3.95
		0.08	0.0807	5.30
		0.10	0.102	6.6
		0.125	0.1239	7.55
		0.14	0.1462	8.30

TABLE 15. Calculation of Integrated Rate Expression as a Function of Residence Time at 195°C

Temp. °C	Mole Ratio $\bar{R}$	Conversion X	$\ln\frac{(\bar{R} - 3X)}{\bar{R}(1-X)}$	W/F gm-cat-hr/ gm-mole
195	40	0.20	0.2079	3.2
		0.25	0.2685	5.45
		0.30	0.334	6.60
		0.35	0.4043	8.15
		0.40	0.4804	8.90
195	50	0.15	0.1534	2.5
		0.30	0.3384	5.75
		0.35	0.4195	6.65
		0.40	0.4863	7.65
		0.45	0.5705	8.6
195	60	0.1	0.1004	1.75
		0.2	0.243	3.5
		0.3	0.3816	5.35
		0.4	0.4906	6.95
		0.5	0.6676	
195	90	0.25	0.2793	3.05
		0.30	0.3466	4.0
		0.35	0.4230	4.68
		4.0	0.4974	5.35
		0.45	0.5811	6.1

TABLE 16. Calculation of Integrated Rate Expression as a Function of Residence Time at 245°C

Temp. °C	Mole Ratio $\bar{R}$	Conversion X	$\ln\frac{(\bar{R} - 3X)}{\bar{R}(1-X)}$	W/F gm-cat-hr/ gm-mole
245	40	0.6	0.8703	4.25
		0.65	0.9999	4.9
		0.7	1.15	5.65
		0.75	1.3285	6.35
		0.80	1.5476	7.75
		0.85	1.8313	8.55
245	50	0.55	0.7649	3.25
		0.60	0.8796	3.75
		0.65	1.01	4.25
		0.7	1.1611	4.85
		0.75	1.3402	5.35
245	60	0.55	0.7707	2.85
		0.65	1.0168	3.80
		0.7	1.1684	4.35
		0.75	1.3481	5.1
		0.8	1.5686	5.8
		0.85	1.8537	6.2
245	90	0.45	0.5827	1.7
		0.5	0.6764	2.0
		0.6	0.8961	2.65
		0.65	1.0278	3.05
		0.75	1.3609	4.0
		0.8	1.5824	4.45
		0.85	1.8684	4.8

TABLE 17. Calculation of Integrated Rate Expression as a Function of Residence Time at 280°C

Temp. °C	Mole Ratio $\bar{R}$	Conversion X	$\ln\frac{(\bar{R} - 3X)}{\bar{R}(1-X)}$	W/F gm-cat-hr/ gm-mole
280	40	0.7	1.15	2.75
		0.75	1.3285	3.15
		0.85	1.8313	4.0
		0.90	2.2327	5.15
		0.95	2.9218	6.75
280	50	0.7	1.1611	2.2
		0.75	1.3462	2.70
		0.8	1.5603	2.95
		0.85	1.8447	3.50
		0.9	2.2471	4.35
		0.95	2.9370	5.8
280	60	0.7	1.1684	1.7
		0.75	1.3481	2.0
		0.8	1.5686	2.32
		0.85	1.8537	2.82
		0.90	2.2566	3.4
		0.95	2.9468	4.5
280	90	0.7	1.1804	1.4
		0.75	1.3609	1.7
		0.8	1.5824	1.95
		0.85	1.8684	2.28
		0.90	2.2721	2.78
		0.95	2.9636	3.2

F-5 Calculation of the overall rate constant at temperature of 145, 195, 245 and 280°C and hydrogen/pyridine molar ratios of 40, 50, 60 and 90.

TABLE 18. Calculation of the Overall Rate Constant

Temp. °C	Mole Ratio $\bar{R}$	$\left[P_{py}^{\circ}\right] 10^4$ N/m^2	$(1/\left[P_{py}^{\circ}\right] \times 10^{-4}$ m^2/N	Slope gm-mole/hr gm-cat	$\left[P_{py}^{\circ}\right] (\bar{R}-3) \times 10^4$ N/m^2	$k_{ov} \times 10^{-8}$ gm-mole/hr gm-cat N/m^2
145	40	6.9942	0.14297	0.00717	258.785	0.27436
145	50	5.6721	0.1763	0.00938	266.588	0.3522
145	60	4.7183	0.21194	0.0108	268.943	0.4016
145	90	3.3056	0.3025	0.014535	287.587	0.50542
195	40	7.1377	0.14010	0.05033	264.095	1.906
195	50	5.55186	0.18012	0.06326	260.937	2.4243
195	60	4.6196	0.216469	0.070716	263.317	2.6856
195	90	3.3001	0.30302	0.09185	287.108	3.1993
245	40	6.8977	0.14497	0.20264	255.21	7.9401
245	50	5.6858	0.175876	0.23309	267.23	8.7198
245	60	4.8943	0.2043	0.26292	278.975	9.4246
245	90	3.3326	0.3	0.33213	289.936	11.4553
280	40	7.3007	0.13697	0.43352	270.126	16.049
280	60	5.4556	0.183297	0.5039	265.413	19.65196
280	80	4.6136	0.21675	0.64668	262.975	24.591
280	90	3.313	0.30184	0.81324	288.23	28.215

F-6 Calculation of activation energy and frequency factor at temperatures of 145, 195, 245 and 280°C.

TABLE 19. Calculation of Activation Energy and Frequency Constant

Mole Ratio $\bar{R}$	T $^{\circ}K$	$1/T \times 10^{-3}$ $^{\circ}K^{-1}$	$k_{ov} \times 10^{-8}$ $\frac{gm\text{-}mole/hr}{gm\text{-}cat\ N/m^2}$	$-\log k_{ov}$
40	418	2.3914	0.27436	19.714
40	468	2.1367	1.906	17.775
40	518	1.9305	7.9401	16.348
40	553	1.8083	16.049	15.645
50	418	2.3914	0.3522	19.464
50	468	2.1367	2.4243	17.535
50	518	1.9305	8.7198	16.255
50	553	1.8083	19.65196	15.442
60	418	2.3914	0.4016	19.332
60	468	2.1367	2.6856	17.432
60	518	1.9305	9.4246	16.177
60	553	1.8083	24.591	15.218
90	418	2.3914	0.50542	19.103
90	468	2.1367	3.1993	17.257
90	518	1.9305	11.4553	15.982
90	553	1.8083	28.215	15.08

G Summary of Results

TABLE 20. Summary of Constants in the Rate Constant Expression

$$k_{ov} = k_s / \left[P_{py}^{\circ}\right] + k_i$$

SUMMARY

Temp.	$+ k_s$ x $\frac{\text{gm-mole/hr}}{\text{gm-catalyst}}$ x 10^{-4}	k_i x 10^{-8} $\frac{\text{gm-mole/hr}}{\text{gm-cat N/m}^2}$
145	1.61788	0.033744
195	7.60346	0.957626
245	22.4762	4.74839
280	74.7421	6.45224

TABLE 21. Summary Activation Energy and Frequency Factor

$$k_{ov} = k_o \exp. (-Ea/RT)$$

Mole Ratio $\bar{R}$	E_a K cal/mole	$k_o \times 10^{-2}$ $\frac{\text{gm-mole}}{\text{gm-cat-hr N/m}^2}$
40	13.909	5.7714
50	13.576	4.863
60	13.763	6.9
90	13.517	6.415

Average E_a = 13.691 K cal/gm-mole

Average $k_o = 5.987 \times 10^{-2}$ $\frac{\text{gm-mole}}{\text{gm-cat-hr N/m}^2}$